

DESIGN OF A SOLAR THERMAL POWERED COOLING SYSTEM

Olli Hurri

Bachelor's Thesis
May 2011

Wellness Technology
Technology, Communication and Transport



JYVÄSKYLÄN AMMATTIKORKEAKOULU
JAMK UNIVERSITY OF APPLIED SCIENCES



Author(s) HURRI, Olli	Type of publication Bachelor's Thesis	Date 11.05.2011
	Pages 95	Language English
	Confidential <input type="checkbox"/> Until	Permission for web publication <input checked="" type="checkbox"/>
Title DESIGN OF A SOLAR THERMAL POWERED COOLING SYSTEM		
Degree Programme Degree Programme in Wellness Technology		
Tutors(s) MATILAINEN, Jorma		
Assigned by Robert Bosch GmbH DANNE, Thomas		
Abstract <p>The main objective of the thesis was to design a mechanical structure for a desiccant evaporative cooling, to apply solar thermal powered air conditioning systems in detached houses. The work was based on a process which was already proven thermally efficient by experimental tests of a prototype. The thesis was carried out in the group "Solar Systems" which belongs to the "Corporate Research" unit of the company Robert Bosch GmbH.</p> <p>In southern Europe, to maintain comfortable inside air conditions, inefficient electronically driven cooling methods are used in a large scale during the relatively hot summers. Simultaneously with high cooling demands, usually intensive solar radiation is present. The desiccant evaporative cooling is a sensible way to utilize the available solar thermal energy in the air conditioning systems, when an electrical cooling coefficient of performance of over 20 can be reached.</p> <p>The most critical factors of the design were pressure loss and size which are related to each other. In general, the desiccant evaporative cooling systems were already in industrial use, but downscaling of the system led to several problems such as unacceptably high internal leakage and pressure drop. Thus, new solutions were needed for the small applications.</p> <p>As an introduction, was an orientation to the thermal process behind the desiccant evaporative cooling. Then, the mechanical design was started with several estimations. During the design process, new construction concepts and mechanical solutions were invented. At the same time, besides the pressure loss, components such as heat exchangers, valves, fans, filters and water spray nozzles were optimized. During the optimization, various engineering tools were used and with each step the estimations of the variables became more precise.</p> <p>The design outcome is a conceptual 3D model of a construction that contains the optimized components of the desiccant evaporative cooling process in the required size. The pressure loss in the construction is calculated comprehensively. Due to that, the most mentionable design result is the proven competitiveness of the desiccant evaporative cooling system for detached house use. Additionally, a noteworthy invention is a simple and effective valve mechanism to control the adsorption and desorption phases, which can be used in nearly every open cycle desiccant evaporative cooling system.</p>		
Keywords solar energy, desiccant evaporative cooling, air ventilation		
Miscellaneous		



Tekijä(t) HURRI, Olli	Julkaisun laji Opinnäytetyö	Päiväys 11.05.2011
	Sivumäärä 95	Julkaisun kieli englanti
	Luottamuksellisuus () saakka	Verkkojulkaisulupa myönnetty (x)
Työn nimi AURINKOJÄÄHDYTYSJÄRJESTELMÄN OMAKOTITALOSOVELLUKSEN SUUNNITTELU		
Koulutusohjelma Hyvinvointiteknologian koulutusohjelma		
Työn ohjaaja MATILAINEN, Jorma		
Toimeksiantaja Robert Bosch GmbH DANNE, Thomas		
Tiivistelmä <p>Kuudessa tunnissa aurinko säteilee maailman aavikoille enemmän energiaa kuin koko ihmiskunta kuluttaa vuodessa. Kesäisin samainen energialähde aiheuttaa epämiellyttävän kuumuuden asuintiloihin esimerkiksi Etelä-Euroopassa. Huolimatta epämiellyttävän kuumuuden ja käytettävissä olevan aurinkoenergian samanaikaisuudesta, asuintiloja jäähdytetään pääasiassa matalahyötysuhteisilla sähköteknologioilla. Globaalien ympäristöongelmien, kuten ilmastonmuutoksen torjunnassa sähkönkulutuksen pienentäminen on avainasemassa. Ilmastoinnin osalta mahdollinen tulevaisuuden ratkaisu kesäisen sähkökuorman alentamiseen on aurinkojäähdytys.</p> <p>Saksassa Robert Bosch GmbH:n tutkimusyksikössä tehdyn opinnäytetyön aiheena oli aurinkoenergiaa hyödyntävän ilmastointikoneen omakotitalosovelluksen suunnittelu. Aurinkojäähdytys perustuu kuivaushaihdutusjäähdytykseen (DEC), joka käyttää auringon lämpöenergiaa kuivausaineen regenerointiin. Aurinkoenergian suoman hyödyn ansiosta tehokas ilmastointi on mahdollista toteuttaa minimaalisella sähkönkulutuksella.</p> <p>Opinnäytetyön suurin haaste oli DEC-prosessia kunnioittavan ja kooltaan omakotitaloon sopivan ilmastointikoneen suunnittelu. Keskeinen ongelma oli vaatimusten mukainen toisistaan riippuvien rakenteen ja painehäviön optimointi. Itse optimointi perustui jäähdytysprosessin ja ilmastointikoneen komponenttien teorian ohella fyysisen rakenteen ideointiin, sekä toiminnallisten komponenttien suunnitteluun koneenrakennuksen ja virtausdynamiikan keinoin.</p> <p>Suunnittelutyön tuloksia ovat ensisijaiset vaatimukset täyttävät 3D-mallit omakotitalosovelluksesta, sekä järjestelmän optimoidut toiminnalliset komponentit. Suunnittelun järjestelmän painehäviö on määritetty kattavasti, jonka perusteella aurinkojäähdytyksellä voidaan saavuttaa sähköinen hyötysuhde noin 29. Lisäksi tuloksena täytyy mainita keksintö venttiilimekanismista, joka mahdollistaa matalahäviöisen ilmavirtojen kontrolloinnin jokaisessa avoimessa DEC-sovelluksessa. Opinnäytetyön tulosten nojalla voidaan aurinkojäähdytys omakotitalosovelluksissa todeta järkeväksi. Lisäksi järjestelmän yksinkertaista rakennetta ja työssä käytettyjä suunnittelulinjoja voidaan käyttää tukevana pohjana varsinaiselle tuotekehitykselle kohti energiatehokasta ilmastointia.</p>		
Avainsanat (asiasanat) aurinkojäähdytys, kuivaushaihdutusjäähdytys, ilmastointi		
Muut tiedot		

CONTENTS

1	INTRODUCTION	5
1.1	Solar energy and cooling	5
1.2	Robert Bosch GmbH and CR/AEB2	7
1.3	Objectives	8
2	THEORETICAL BACKGROUND	10
2.1	Basic elements of desiccant evaporative cooling	10
2.1.1	Heat exchanger	10
2.1.2	Adsorption	13
2.1.3	Evaporative cooling	15
2.2	Solar thermal powered desiccant evaporative cooling	17
2.2.1	Desiccant evaporative cooling	17
2.2.2	Process values	19
2.2.3	Winter mode	22
2.3	Pressure loss calculation	23
2.3.1	Empirical method	25
2.3.2	Computational fluid dynamics	27
2.4	Fans	29
2.5	Filters	34
2.6	Water hydraulics	37
3	DESIGN PROCESS	39
3.1	First stage	39
3.1.1	Requirement list and objectives	39
3.1.2	Efficiency estimations	40
3.1.3	Valve mechanism to control air flows	42
3.1.4	First construction	46
3.2	Second stage	49
3.2.1	Fan design	49
3.2.2	Applying indirect evaporative cooling to the cooling box	52
3.2.3	Second construction	53
3.2.4	Optimization of valve mechanism	56

3.3 Third stage 58

 3.3.1 Filters 58

 3.3.2 Water cycles 60

 3.3.3 Third construction 62

 3.3.4 Pressure loss and power consumption 64

4 CONCLUSION 66

REFERENCES 69

APPENDICES 72

 Appendix 1. Requirement list 72

 Appendix 2. Coated heat exchangers 74

 Appendix 3. Cross counter flow heat exchanger 75

 Appendix 4. Efficiency estimations 76

 Appendix 5. Initial setup possibilities 77

 Appendix 4. Competitors technical data 78

 Appendix 7. RadiCal fans 79

 Appendix 8. Beam torque optimization 81

 Appendix 9. Beam bending flexure optimization 83

 Appendix 10. Pressure drop in fibrous filters 85

 Appendix 11. Water cycles 87

 Appendix 12. Pressure loss in cooling box 89

 Appendix 13. Pressure loss in third construction 90

 Appendix 14. Computational pressure loss 94

FIGURES

FIGURE 1. Domestic loads and solar gains in southern Europe 7

FIGURE 2. Overall energy balance of counter flow heat exchanger 11

FIGURE 3. Finned tube heat exchanger 12

FIGURE 4. Movements of molecules in adsorption and desorption 13

FIGURE 5. Macro- and micro-porosity of adsorbent 14

FIGURE 6. Sorption material load of silica gel 15

FIGURE 7. Direct and indirect evaporative cooling 16

FIGURE 8. Coated heat exchanger concept 18

FIGURE 9. Process values of the DEC 20

FIGURE 10. Winter mode and bypass valve 22

FIGURE 11. Laminar and turbulent flow 23

FIGURE 12. Flow development. 25

FIGURE 13. Structure of centrifugal fan 30

FIGURE 14. Shapes of impeller blades 30

FIGURE 15. Fan curves 33

FIGURE 16. Ways of particle collection 35

FIGURE 17. Factors of filter design 36

FIGURE 18. Functional parts of centrifugal pump 37

FIGURE 19. Symbol of required valve 43

FIGURE 20. Principles of the valve mechanism 43

FIGURE 21. Back and front view of valve mechanism 44

FIGURE 22. Sheet metal plates 45

FIGURE 23. Fan box and back flow valve 46

FIGURE 24. First construction 47

FIGURE 25. RadiCal fan and EC power. 50

FIGURE 26. Compact module and scroll housing 51

FIGURE 27. Direct and indirect cooling box 52

FIGURE 28. Second construction 54

FIGURE 29. Valve mechanism driven by electric cylinder 56

FIGURE 30. Solid and hollow beam 57

FIGURE 31. Filter setup 59

FIGURE 32. Size optimization for filters. 60

FIGURE 33. Third construction 63

TABLES

TABLE 1. Fan laws 32

TABLE 2. Pressure drop in filter elements 60

TABLE 3. The total power consumption of the fans 65

TABLE 4. The total electric cooling efficiency 65

Nomenclature and abbreviations

Symbol	Definition	Unit	Subscript	Definition
A	area	m^2	1, 2, 3. . .	operating point
a	speed of sound	$\frac{m}{s}$		section
α	solidity	-	A, B	section
α, β, \dots	angle	$^\circ$	<i>adsorbate</i>	adsorbate material
B, b	width	m	<i>adsorbent</i>	adsorbent material
C	Cunningham slip correction factor	-	<i>air</i>	room air material
C_k	local loss coefficient	-	b	beam (rotary valve slide)
COP	coefficient of performance	-	c	cold medium
$C_{sorption}$	sorption material load	-	<i>cold</i>	cooling effect
c_p	specific heat capacity	$\frac{J}{K \cdot kg}$	<i>complete</i>	complete system
D, d	diameter	m	<i>components</i>	loss in components
	depth	m	<i>cooling</i>	cooling process
	bending flexure	m	d	diffusion
	diffusion coefficient	-	<i>dry</i>	dry material
E	Young's modulus	GPa	<i>dynamic</i>	dynamic effect
ε	kinematic dissipation rate	-	e	end condition
ε_d	surface roughness	mm	<i>electric</i>	electricity of system
F_c	force of cylinder	N	<i>facing</i>	facing condition
F_{feed}	feed force	N	<i>fan</i>	fan unit
f	Darcy friction factor	-	<i>filter</i>	filter element
	frequency	Hz	<i>friction</i>	friction loss
G	static gravity load	$\frac{N}{m}$	H	hydraulic
g	gravity	$\frac{m}{s^2}$	H_2O	water
g_x, g_y, g_z	orientation of gravity	-	h	hot medium
H, h	height	m	<i>hollow</i>	hollow structure
	delivery height	m	i	initial condition
	specific enthalpy	$\frac{kJ}{kg}$	<i>local</i>	local loss
η	efficiency	-	<i>motor</i>	motor unit
ϑ	temperature	$^\circ C; K$	<i>partial</i>	partial condition
I	electric current	A	<i>particle</i>	property of average particle
I_y	second moment of inertia, y-axis	m^4	<i>solar</i>	solar thermal system
Ku	Kuwabara number	-	<i>solid</i>	solid structure
k	overall heat transfer coefficient	$\frac{W}{m^2 \cdot K}$	<i>standard</i>	standard ventilation
	turbulence kinematic energy	$\frac{m^2}{s^2}$	<i>static</i>	static effect
k_B	Boltzmann's constant	$\frac{J}{K}$	<i>thermal</i>	thermal system
L	length	m		
L_p	sound pressure level	dB	Abbreviation	Definition
λ	mean free path of air molecule	m	AC	alternate current
M	Mach number	-	CFD	computational fluid dynamics
	molecular mass	$\frac{g}{mol}$	DC	direct current
	torque	Nm	DEC	desiccant evaporative cooling
m	mass	kg	EC	electronically controlled current
\dot{m}	mass flow	$\frac{kg}{s}$	FEM	finite element method
μ	dynamic viscosity	$\frac{kg}{s \cdot m}$	HX	heat exchanger
n	rotation speed	$\frac{1}{s}$	IEC	indirect evaporative cooling
n_{waves}	number of waves	-		
ν	kinematic viscosity	$\frac{m^2}{s}$		
P	power	W		
Pe	Peclet number	-		
P_{wetted}	wetted perimeter	m		
p	pressure	Pa		
ρ	density	$\frac{kg}{m^3}$		
Q	volumetric flow	$\frac{m^3}{s}; \frac{m^3}{h}$		
Q	heat flux	$\frac{W}{m^2}$		
q	static load	$\frac{N}{m}$		
R	interception parameter	-		
Re	Reynolds number	-		
r	radius	m		
s	stroke of cylinder	m		
U	voltage	V		
u	mean velocity	$\frac{m}{s}$		
u, v, w	velocity in x, y, z-axis direction	$\frac{m}{s}$		
V	volume	m^3		
x	specific humidity	$\frac{g}{kg}$		
x, y, z	position in coordinate system	m		
Z	thickness	m		

1 INTRODUCTION

1.1 Solar energy and cooling

The most important energy supplier of Earth is the sun. It provides light and heat and thereby enables life on earth. In addition to that, the sun is the most environmentally friendly and continuous source of energy. Available solar energy is 1.5×10^{18} kWh per annum, which is more than 10000 times current energy demand of the world (Planning and installing solar thermal systems, 2010, p. 11). The maximum intensity of solar irradiation on the surface of earth can be over $1000 \frac{W}{m^2}$ but it is difficult to exploit for our purposes (Eck, 2008, p. 28).

“Within 6 hours deserts receive more energy from the sun than humankind consumes within a year” (Knies, n.d.).

In the year 2008 over 80 % of our energy was produced by burning fossil fuels (Key World Energy Statistics 2010, 2010, p. 6). By burning fossil fuels, greenhouse gases such as carbon dioxide and methane are released to the atmosphere. These greenhouse gases are intensifying the natural greenhouse effect and are causing global warming. Global warming describes the increase of average temperature on the surface of earth in long-term statistics. It is noted as a major part of climate change. According to the present consensus of scientist, a large part of this climate change is caused by human activities (Advancing the science of climate change, 2010, p. 1).

Climate change concerns the whole world and various decisions are made to cut the greenhouse gas emissions. The most well-known decision took place when the European Union ratified the Kyoto Protocol to the United Nations Framework Convention on Climate Change (UNFCCC). Within the European Union every country in the world besides the United States has ratified the Kyoto Protocol (Status of Ratification of the Kyoto Protocol, 2011). The Kyoto protocol is a long-term commitment to maintain our environment and its main target is to reduce overall greenhouse gas emissions to at least 20 % of 1990 levels by the year 2020 (Directive 2010/31/EU, 2010, p. L153/13).

To match with the objectives of the Kyoto protocol, in the Directive 2010/31/EU of European Parliament and the Council it is legislated that “by 31 December 2020, all new buildings are nearly zero- energy buildings”. To meet these targets in practice, the use of renewable energy sources has to be increased where as overall energy consumption needs to be reduced. In the European Union, buildings account for 40 % of the total energy consumption which means that with new solutions in the building sector, huge energy saving potential can be exploited (Directive 2010/31/EU, 2010, p. L153/21).

Due to the huge energy potential, the sun is one of the most interesting source of renewable energy. Currently, the two main ways to use solar energy are photovoltaic and solar thermal collectors. Photovoltaic means that electromagnetic radiation from the sun is converted into a direct current in the cells of the solar panel. This way, the collected energy can be used for electrical devices. In general, the electricity is fed into the electric grid. To collect solar thermal energy, water is pumped through solar thermal collectors. Sensible heat can be stored in isolated water tanks and can be used for example as a source of heat for domestic water or floor heating.

Although the sun is constantly radiating with approximately the same intensity, environmental conditions on earth are changing continuously. The earth is moving in an orbit around the sun, and at the same time, rotating around its own nearly vertical axis. These movements are creating different times of day, seasons and weather on earth. In the summer, solar radiation in southern Europe is relatively high. For example, the average highest temperature of the day in Italy is 28.6°C during July (Weather Information for Rome (ROMA), 2011).

Hot outside conditions are also causing a rise of inside temperature. Most of the people are experiencing inside temperatures higher than 26°C or relative humidity higher than 65 % uncomfortable (DIN 1946-2, 1994, p. 3). To cool the air down, inefficient electric cooling processes are commonly used in residential buildings. Solar thermal powered cooling process which is discussed in this thesis, offer an environmentally friendly and effective solution to ensure cool and dry air in buildings during the summer. In the summer when a need for cooling is highest, solar radiation is also highest, which makes solar cooling rather sen-

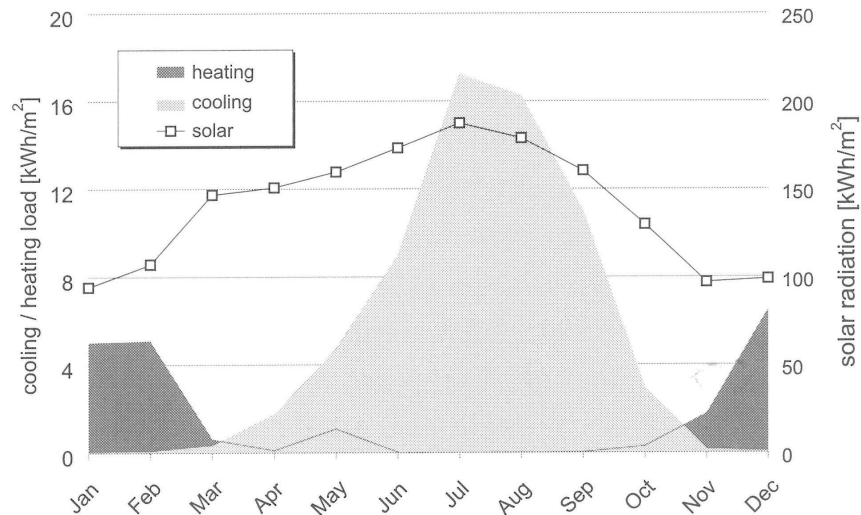


FIGURE 1. Domestic loads and solar gains in southern Europe (Henning, 2004, p. 2).

sible (see Figure 1). Solar thermal powered cooling systems are already in use in some industrial buildings, but systems for detached house use are still under development.

1.2 Robert Bosch GmbH and CR/AEB2

In 1886 Robert Bosch (1861-1942) founded his company as “Workshop for Precision Mechanics and Electrical Engineering” in Stuttgart, Germany (Robert Bosch: His life and work, 2011, pp. 28-31). The ongoing industrialization in Europe set a high demand for the development of new technical components. Bosch was strongly involved in this and huge steps were taken especially in automotive technology. As a result Bosch’s high voltage magneto gave the first spark in a combustion chamber in 1902 (Facts and Figures, 2011, p. 28).

Nowadays Bosch is operating in the areas of automotive and industrial technology, consumer goods, and building technology. The Bosch Group is a worldwide operating company, represented in 150 countries. In fiscal the year 2009, 275.000 employees of the Robert Bosch GmbH generated a turnover of 38,2 billion euros. 92 % of the share capital of the Robert Bosch GmbH is owned by the charitable foundation Robert Bosch Stiftung GmbH. This special ownership offers stable ground for effective and long-term research. Every year, an investment of 3,6 bil-

lion euros into research leads to approximately 3800 patents (Bosch Today, 2010, p. 9).

Environmentally friendly and energy efficient solutions are becoming more important. Bosch as a huge technology supplier also has high intention and responsibility to take care of the environment and to find sustainable energy solutions. The most known environmental milestones are reached under Bosch's "Invented for Life" theme in automotive technology. For example, efficient injection and electricity solutions are widely used in new cars. Furthermore, Bosch solar systems are ranked among the most efficient solar applications of the world, which gives a high push for research with renewable energy sources (Facts and Figures, 2011, p. 10).

This thesis is carried out in the group CR/AEB2 which stands for "Solar Systems". CR/AEB2 is part of the department "Future Systems in Building Technology" which belongs to the division "Future systems for Industrial Technology, Consumer Goods and Building Technology" (CR/AE3). In larger scale CR/AEB2 is part of Bosch's "Corporate Research", where all initial research is done. CR/AEB2 is co-operating with the Bosch Thermotechnik GmbH (thermotechnology) which is taking care of product management and therefore of any further actions of the results obtained in CR/AEB.

1.3 Objectives

The main task of this thesis is to develop, analyze and optimize design concept of a solar thermal powered air conditioning system for detached house use. Thermodynamic inventions are offering various opportunities to utilize different energy sources in buildings. One of these inventions is solar thermal powered air conditioning systems. These systems, as part of modern building technology, provide help in getting closer to the zero-energy house of the future and highly support the use of sustainable energy sources and ensure comfortable inside air quality.

Until now, two prototypes with different desiccant evaporative cooling methods have been under testing and developing. The methods used are so called DEC (desiccant evaporative cooling) processes, one with a liquid and one with solid sorbent. Both prototypes are working effectively, even though the process parameters are still not optimized. By connecting these prototypes to a simulation system, which can generate different outside and discharged air conditions, high potential of desiccant evaporative cooling is found. Similar solar thermal powered air conditioning systems are already in use in some industrial buildings and high electrical efficiencies are reached. The next step is to design a construction for solar thermal powered air conditioning system which can be installed into a detached house and which can be used as a source for high quality inside air.

The intended use of the concept in detached houses is setting many requirements for the design. The design has to be done with respect to the size limitations and process values. The system has to be almost like any existing air conditioning system, with sensible price and without any compromises in efficiency and air quality.

The main objective of this thesis is to find out what an actual product could look like. According to the state of the project as a result of the design work, conceptual 3D models are sufficient. During the way from the first idea to the actual product on this level of development, it is important to prove competence or incompetence of the whole system. The applied thermal process is proved effective and working by previous and ongoing researches (Kübler, 2010).

The most critical points for the construction are:

- Physical size limits must not be exceeded
- Low pressure loss to meet efficiency requirements

If these specifications can be met, it proves that it is sensible to continue with the development of such a system.

2 THEORETICAL BACKGROUND

In this chapter, the theoretical background concerning the desiccant evaporative cooling (DEC) and the actual design work is explained. To ensure proper design, it is important to understand the main functions of the DEC process. Hence, a relatively huge part of this chapter is connected to the DEC process itself. First, the basic thermodynamic components and processes which are utilized for the DEC process are explained. In 2.2 different functions of the cooling process are discussed step by step, and a theoretical setup of the components needed is shown. Experimental process values and estimated cooling performance based on collected data from previous tests are given. Rest of the theory is concerns the tools of design work used in this thesis and for the component selection. The design tools used are mostly connected to the fluid dynamics. A background in the fluid dynamics is important in order to estimate the pressure drop, which is the most critical factor for the electric consumption. Furthermore, background information about fans and filters is given.

2.1 Basic elements of desiccant evaporative cooling

In this section, important thermodynamic components and processes for the DEC cycle are discussed. Heat exchangers are discussed because they are widely used in the DEC process. Furthermore, basics of adsorption and evaporative cooling are clarified as they are assumed to be advanced knowledge.

2.1.1 Heat exchanger

A heat exchanger (HX) is a piece of equipment which enables continuous heat transfer between separated mass flows. A heat exchanger is based on the zeroth law of thermodynamics, which defines that heat transfer from higher temperatures to lower temperatures occurs until equilibrium in the system is reached. In the heat exchanger, mixing of two mass flows is prohibited by heat conductive material. The heat transfer (heat flux) in the heat exchanger is based on the

heat conduction through the heat conductive material as well as the heat transfer between the two mass flows due to forced convection. Therefore, heat flux \dot{Q} in the heat exchanger is mainly dependent on the internal surface area A and the overall heat transfer coefficient k which incorporates the heat transfer in the two flows and the conduction in the material. The heat flux \dot{Q} given in Equation 1 and efficiency $\eta_{thermal}$ given in Equation 2 (Böckh, 2006, pp. 207-231).

$$\begin{aligned}\dot{Q} &= k * A * \left(\frac{(\vartheta_{h,i} - \vartheta_{h,e}) - (\vartheta_{c,e} - \vartheta_{c,i})}{\ln((\vartheta_{h,i} - \vartheta_{h,e}) / (\vartheta_{c,e} - \vartheta_{c,i}))} \right) \\ &= -(\dot{m}_h * c_{p,h}) * (\vartheta_{h,e} - \vartheta_{h,i}) \\ &= (\dot{m}_c * c_{p,c}) * (\vartheta_{c,e} - \vartheta_{c,i})\end{aligned}\quad (1)$$

$$\begin{aligned}\eta_{thermal,c} &= \frac{(\vartheta_{c,e} - \vartheta_{c,i})}{(\vartheta_{h,i} - \vartheta_{c,i})} \\ \eta_{thermal,h} &= \frac{(\vartheta_{c,e} - \vartheta_{c,i})}{(\vartheta_{h,i} - \vartheta_{c,i})}\end{aligned}\quad (2)$$

In the Equations 1 and 2 symbol ϑ stands for temperature, c_p for heat capacity, \dot{m} for mass flow, subscript h for hot fluid, subscript c for cold fluid and subscripts i and e for initial and end condition. Overall energy balances of a heat exchangers are shown in Figure 2.

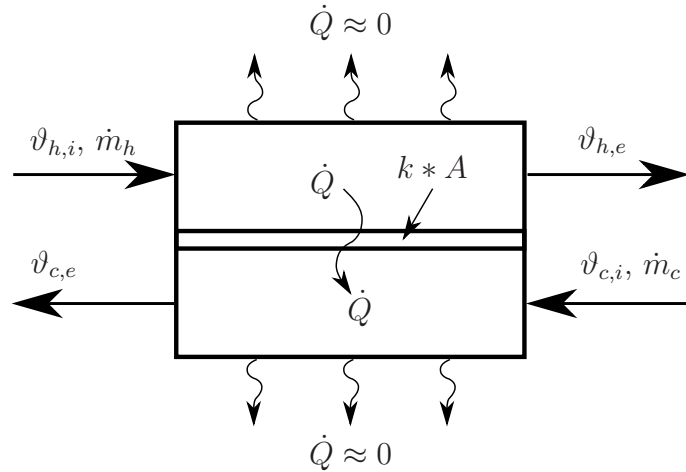


FIGURE 2. Overall energy balance of counter flow heat exchanger (based on Böckh, 2006, p. 207).

The structure of the heat exchanger depends on the desired mass flows and efficiency. Heat exchangers are classified by the states and directions of used mass flows. Heat exchangers are mostly applied to processes where gas-to-gas, gas-to-liquid or liquid-to-liquid heat transfer is needed. In general, different directions

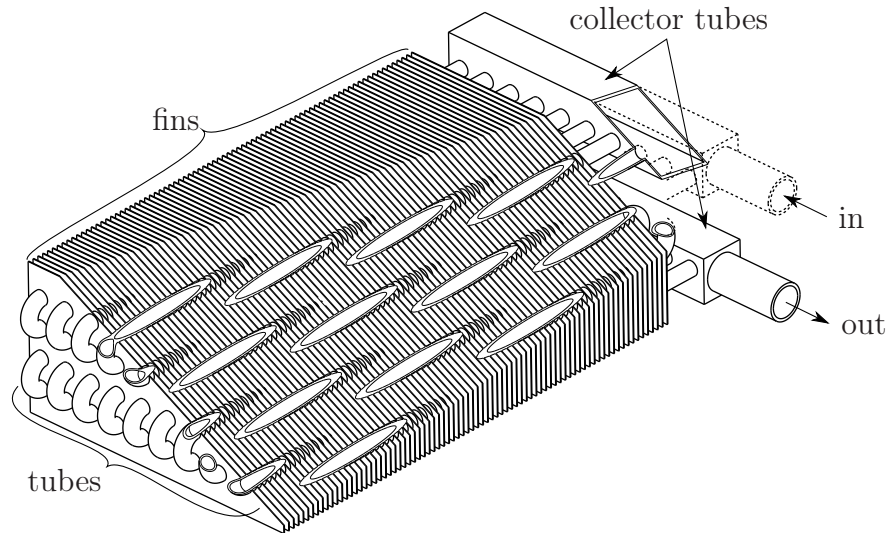


FIGURE 3. Finned tube heat exchanger.

of the mass flows are possible such as parallel, counter, cross and cross counter flow. Additionally, heat exchangers can still be divided by general mechanical structure into tubular and plate heat exchangers or combined construction such as finned tube heat exchanger. All the heat exchangers discussed in this thesis are various types of finned tube heat exchangers, see Figure 3.

In theory, heat exchangers can be applied to any heat transfer process between mass flows. In theory, with a cross flow heat exchanger and infinite internal heat transfer surface area, efficiency of 100 % can be reached. The heat exchangers can be designed freely with respect to dimension and can be implemented in any shape. The only requirement is to keep the internal surface area optimized with respect to the volume of heat exchanger and the pressure drop in it. By increasing the internal surface area and by complicating the internal structure, the pressure drop also increases. Therefore, reaching the optimized point for the thermal efficiency and the pressure drop is important.

In the gas-to-gas heat exchange process, with a cross counter flow heat exchanger thermal efficiency up to 90 %, and a relatively low pressure drop can be reached. In liquid-to-gas processes finned tube cross flow heat exchangers are preferred. In the finned tube heat exchangers the number of the water tubes and the surface area of conduction are maximized, which leads to high efficiency while keeping the volume and pressure drop low.

2.1.2 Adsorption

Adsorption is one of the main processes in DEC cycle. Adsorption means an adhesion of fluid or gas molecule to the surface of the solid material, the so-called desiccant. An accumulating molecule is called adsorptive, an accumulated molecule is adsorbate and the desiccant is adsorbent (see Figure 4). During adsorption, the desiccant stays dimensionally stable during the process, which is the main difference to the similar process, called absorption. The sorption material load $C_{sorption}$ is the ratio between the mass of adsorbate $m_{adsorbate}$ and the dry mass of adsorbent $m_{adsorbent}$ and it is used to describe the status of the desiccant.

$$C_{sorption} = \frac{m_{adsorbate}}{m_{adsorbent}} \quad (3)$$

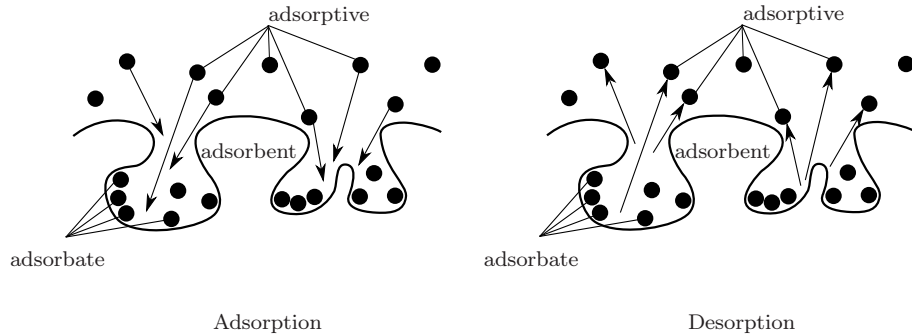


FIGURE 4. Movements of molecules in adsorption and desorption (according to Henning, 2009, p. 58).

In the Langmuir model for adsorption, the formation of a monolayer of the adsorptive molecules on the surface of the adsorbent is assumed (Langmuir, 1916). After an infinite time, the temperature of adsorptive and adsorbent is equal, and the dynamical equilibrium between adsorptive and adsorbate molecules is reached. In conclusion, the sorption material load $C_{sorption}$ in equilibrium state is only dependent on the temperature ϑ and the partial pressure $p_{partial}$ of the adsorptive vapor.

$$C_{sorption} = f(\vartheta, p_{partial}) \quad (4)$$

The equilibrium state can be shifted by adjusting temperature and partial pressure of the adsorptive vapor. By increasing the temperature of the adsorbent or decreasing partial pressure of the adsorptive vapor, reverse function of adsorption starts. This process, when the adsorbent donates adsorbate molecules is called desorption and is used to regenerate adsorbent. In a DEC system, the air used for desorption has a humidity ratio which is given by the operating conditions. Hence, the partial pressure of water vapor is fixed. Therefore state of equilibrium can be controlled only by the temperature of the adsorbent.

Adsorption can be explained with three physical phenomenon. Firstly, the hydrophilic force enables the adhesion of the adsorbate molecule on the surface of the adsorbent. Secondly, the Van Der Waals force between adsorbate molecules enables adhesion for many other adsorbate molecules. Thirdly, the capillary action forces adsorbate molecules into the micro-porous structures (Oertel, 2001, p. 16).

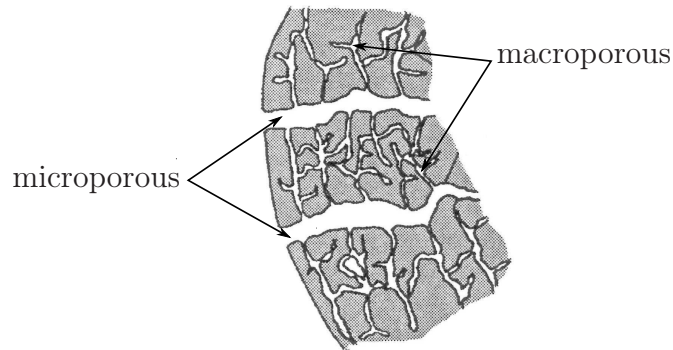


FIGURE 5. Macro- and micro-porosity of adsorbent (Kast, 1988).

The surface structure of the desiccant is porous. The macro- and micro-porous structure of the desiccant (see Figure 5) offers a large surface for the adsorptive molecules to attach. Therefore, porosity is the main feature of the adsorbent. Commonly known adsorbents are activated coal, lithium compounds, silica gel and zeolites. In DEC systems, mainly silica gel and zeolites are used as a coating in heat exchangers and desiccant wheels, because both are dimensionally stable in a wide temperature range. Sorption material load $C_{sorption}$ of silica gel can be given as a function of temperature and relation with the surrounding pressure. In Figure 6 an example of behavior of silica gel is shown under two constant relative pressures. From Figure 6 it follows that the amount of adsorbed water

in silica gel is changing significantly in a relatively small temperature range of 70 K.

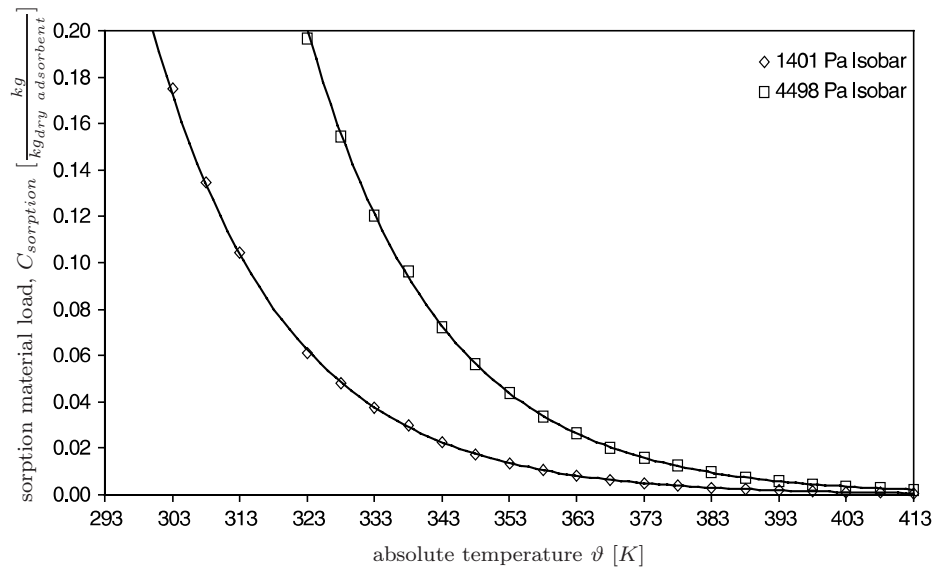


FIGURE 6. Sorption material load of silica gel (according to Ng et al., 2001, p. 1641).

2.1.3 Evaporative cooling

Evaporation is the main mechanism at work to cool down the air in DEC systems. Evaporation is a type of vaporization and the reverse function of condensation. It can occur over the complete temperature range, whenever gas flows over the liquid. When evaporation occurs, the surface layer of the liquid phase of a substance, such as water, changes its phase to gaseous. Evaporation can be explained by the movements of molecules. The movement of the gas molecules due to the temperature accelerates the liquid molecules near the surface and liquid molecules experience collisions between each other. Consequently the energy of the molecules increases above the surface binding energy and liquid molecules evaporate (Incropera and DeWitt, 1996, pp. 325-327).

To continue evaporation on the surface, internal energy from the liquid is required. Hence, the liquid cools down. As steady-state conditions have to be maintained, the latent energy loss of the evaporation is substituted by an energy transfer from the surroundings to the liquid.

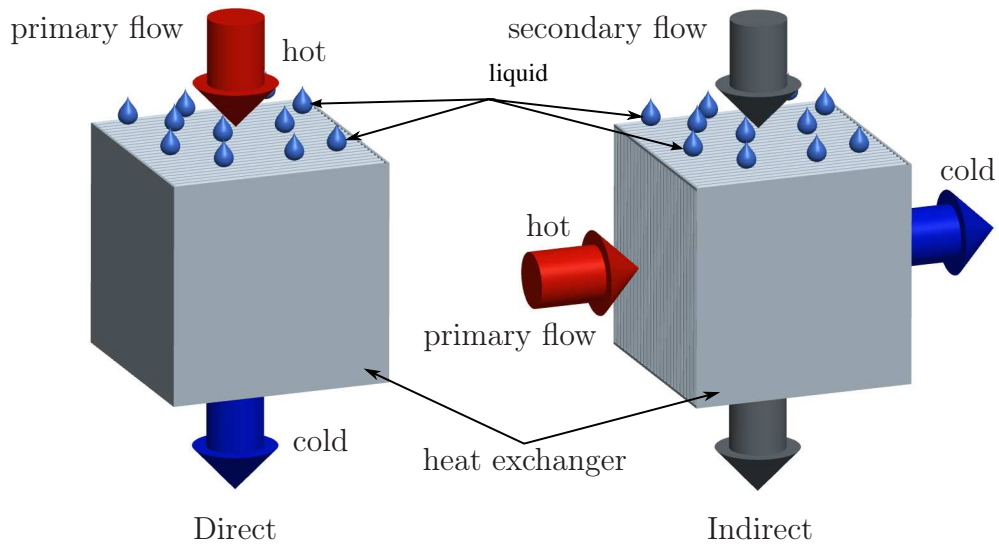


FIGURE 7. Direct and indirect evaporative cooling.

For direct evaporative cooling of air with water, the primary air flow and the water itself are cooled down by allowing free heat and mass transfer. For indirect evaporative cooling (IEC), only heat transfer between the primary air flow and the secondary air flow, in which water is sprayed, is wanted (see Figure 7). The mass flow between the main flow and the secondary flow is prohibited by a material with high thermal conductivity for example heat exchanger, thus the cooling stays effective.


The cooling efficiency is related to the evaporation efficiency. The evaporation efficiency depends on the surface area of the evaporating liquid and the surrounding conditions. On a larger surface area, more molecule collisions are occurring and the evaporation efficiency is increasing. When air flows over water, the most informative factor of the surrounding conditions is relative humidity. Relative humidity is conducted from specific humidity which is based on the ideal gas law. Relative humidity is defined by the ratio of the mass of the water compared to the maximum amount of water vapor that can be held in the constant air volume at the current temperature. With lower relative humidity of the air, evaporation is more effective. In DEC systems, indirect evaporative cooling is easy to achieve in a heat exchanger where the surface area is large and the heat conductivity is high.

2.2 Solar thermal powered desiccant evaporative cooling

Various solar thermal powered air conditioning systems are known. According to the implemented technologies, these systems can be divided into open cycle and closed cycle systems. In an open cycle system (also called desiccant evaporative cooling, DEC) the supply air for the building is dehumidified by using various liquid and solid adsorbents. In a so called adsorption phase the adsorbent adsorbs moisture from the air and afterwards the air is cooled down by indirect evaporative cooling. After the adsorption phase, the sorption capacity of the adsorbent is exhausted and it has to be regenerated in a so called desorption phase. In this phase, solar thermal heat is used for regeneration. The general principle of the specific DEC process embraced in this thesis is discussed in 2.2.1. In 2.2.2 typical process values, such as cooling power are presented. In 2.2.3 the possibility for a heat recovery in winter mode of such a system is presented.

2.2.1 Desiccant evaporative cooling

[Text deleted due to confidentiality]




9Z__thesis_002_pictures_006_aqsoa_process.eps

FIGURE 8. Coated heat exchanger concept.

[Text deleted due to confidentiality]

2.2.2 Process values

[Text deleted due to confidentiality]



10Z__thesis_002_pictures_007_ideal_cooling_process.eps

FIGURE 9. Process values of the DEC.

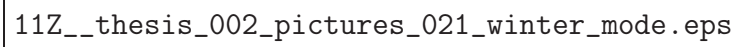
[Text deleted due to confidentiality]

[Text deleted due to confidentiality]

[Text deleted due to confidentiality]

2.2.3 Winter mode

[Text deleted due to confidentiality]



11Z__thesis_002_pictures_021_winter_mode.eps

FIGURE 10. Winter mode and bypass valve.

2.3 Pressure loss calculation

In physics, fluid dynamics is a branch of fluid mechanics where movements of a flowing fluid are under consideration. Every fluid has a density and viscosity which are causing friction and resisting movements. In general, these properties are converting kinematic energy of the fluid to thermal energy which occurs as a pressure drop and increase in temperature of the fluid. Fluid dynamics, especially turbulent fluid flow, contain still unsolved questions and fluid flow situations can be predicted more or less precisely with different methods. In this thesis, two main ways to approach pressure loss of fluid flow include an empirical and a numerical method. The empirical method is to apply factors of measured fluid flow situations into the current situation under inspection. The numerical method is based on computational fluid dynamics, where an advanced calculation power of the computers is utilized. Nonetheless, both methods are based on the same physical background which is discussed in this chapter.

Density ρ stands for the relation between the mass and volume of the fluid, and has unit $\frac{kg}{m^3}$. Viscosity of the fluid describes the ability of the fluid to resist movements. In ordinary life viscosity is called the "thickness" of the fluid. Thus, a fluid with a low viscosity, such as water, is called "thin" and a fluid with a high viscosity, such as syrup is called "thick". In the SI-system viscosity is divided into a dynamic viscosity, whose symbol is μ and unit is $Pa * s (= \frac{kg}{s * m})$, and a kinematic viscosity whose symbol is ν and unit is $\frac{m^2}{s}$. In general, both describe the same property of the fluid but the dynamic viscosity is more often used. The kinematic viscosity is the dynamic viscosity divided by the density of the fluid.

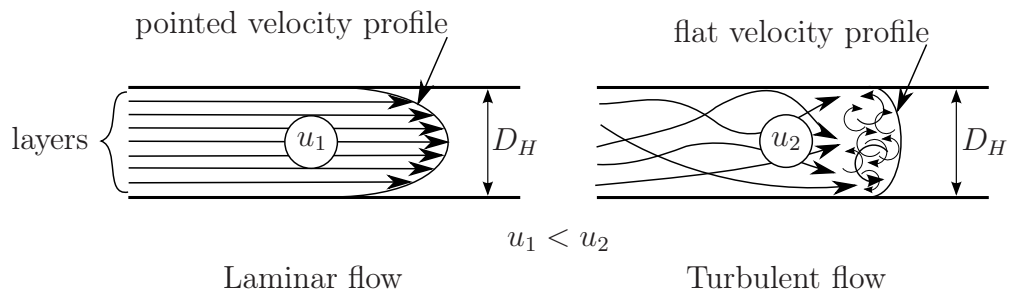


FIGURE 11. Laminar and turbulent flow (according to White, 2003, p. 330, 346).

Fluid flow can be laminar or turbulent, or transitional flow between laminar and turbulent phases (see Figure 11). When the flow is laminar, an internal viscosity force is strong enough to keep movements of the molecules in a stable direction and the fluid flows smoothly in layers. By increasing the velocity of the fluid, the internal viscosity force is exceeded and molecules start to fluctuate. This fluctuation breaks the layers and the flow changes to turbulent. In the turbulent flow, molecules are moving randomly in various directions and pressure loss is higher than in laminar flow. To describe the flow, the dimensionless Reynolds number Re is used. It is given by (see Equation 5) correlation of the mean velocity u multiplied the hydraulic diameter D_H and the dynamic or kinematic viscosity.

$$Re = \frac{\rho * u * D_H}{\mu} = \frac{u * D_H}{\nu} \quad (5)$$

In circular pipes, the hydraulic diameter is the inside diameter of the pipe. In non-circular pipes, hydraulic diameter D_H is 4 times a cross sectional area A of the flow divided by wetted perimeter P_{wetted} (see Equation 6).

$$D_H = \frac{4 * A}{P_{wetted}} \quad (6)$$

Incompressible flow in pipes is laminar, when $Re \leq 2300$, transitional when $2300 < Re < 4000$ and turbulent when $4000 \leq Re$ (Çengel, 2008, p. 608). Flow is incompressible when the Mach number is less than 0,3 (White, 2003, p. 176). The Mach number M is given by:

$$M = \frac{u}{a} \quad (7)$$

Where a stands for a speed of sound in the material under consideration. Generally, in all natural flows and ventilation systems the Mach number is significantly less than 0,3. Thus all flows in this thesis can be assumed incompressible.

When the cross section of a flow channel is changing, the fluid flow also has to adjust to new conditions. For example, after an entrance, boundary layers of the

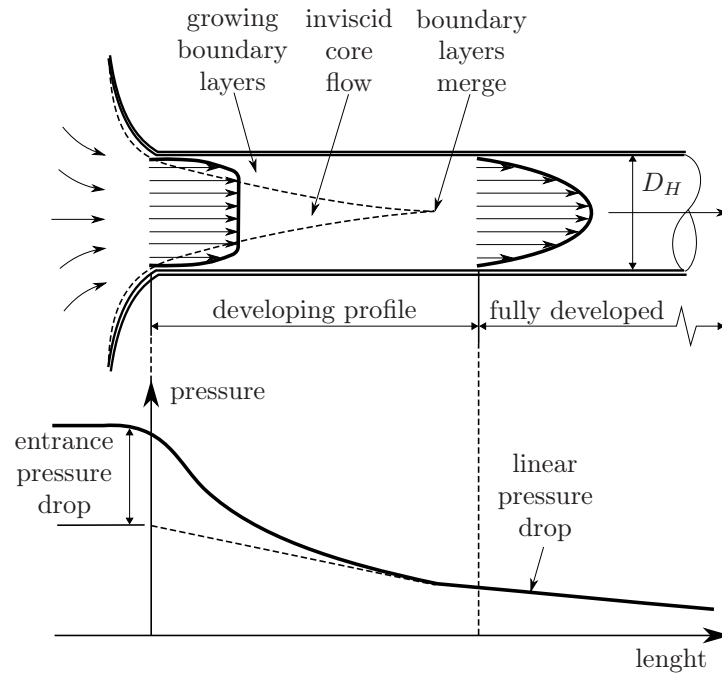


FIGURE 12. Flow development (according to White, 2003, p. 331).

flow are separated by the so-called inviscid core, which is decreasing as a function of channel length (see Figure 12). In the inviscid core, the fluid behaves without viscosity. According to this behavior, the pressure drop of the entrance during the flow development is difficult to predict. When fluid is in a fully developed state, the pressure loss is linear and calculations with empirical formula lead to precise results (White, 2003, pp. 325-333). In ventilation systems, air flow is always strongly turbulent and its structure is complicated. Hence, comprehensive results in the pressure loss calculations are difficult to reach. On the other hand, a percentage of the pressure loss of the structure is assumed to be relatively small in comparison to the pressure loss caused by functional components. This will be shown in the pressure loss calculation of the last construction.

2.3.1 Empirical method

The empirical method to approach pressure loss is to apply measured values in the current system under consideration. The empirical method is deemed valid only for a fully developed flow. Especially in various structures of ventilation unit, the flow is never fully developed. Hence, the reference values never match

exactly and generalizations and structure simplifications are needed. Nonetheless, a relatively precise magnitude of the pressure loss can be achieved.

In the empirical method, the main idea is to use calculated factors for the static friction pressure losses $\Delta p_{friction}$ caused by the walls of air channels. Additionally, local pressure losses Δp_{local} can be calculated by using measured local loss coefficients for elbows, expansions, contractions, entries, exits, transitions and junctions. Furthermore, to reach the total pressure loss, pressure loss caused by functional components $\Delta p_{components}$ has to be added. The total pressure loss Δp_{total} in ventilation unit is given by:

$$\Delta p_{total} = \sum \Delta p_{friction} + \sum \Delta p_{local} + \sum \Delta p_{components} \quad (8)$$

To calculate the frictional pressure loss, the Darcy-Weisbach equation can be used. Darcy-Weisbach equation is written in terms of pressure loss, where friction loss $\Delta p_{friction}$ is given by:

$$\Delta p_{friction} = f * \frac{L}{D_H} * \frac{\rho * u^2}{2} \quad (9)$$

Where L is the length of the pipe under inspection, ρ the density, u the mean velocity f the Darcy friction factor. The Darcy friction factor is calculated iteratively by applying the Colebrook equation given in Equation 10. It is valid if $\frac{65 * D_H}{\varepsilon_d} < Re < \frac{1300 * D_H}{\varepsilon_d}$ (Grote and Feldhusen, 2007, p. B 49).

$$\begin{aligned} \frac{1}{\sqrt{f}} &= -2 \log_{10} \left(\frac{\varepsilon_d / D_H}{3,7} + \frac{2,51}{Re * \sqrt{f}} \right) \\ \Rightarrow f &= \frac{1}{2 * \log_{10} (2,51 / (Re * \sqrt{f}) + 0,27 / (D_H / \varepsilon_d))} \end{aligned} \quad (10)$$

Where ε_d is the roughness of the inside surface of the pipe. The roughness is given for different materials and for technically smooth materials, such as sheet metals, a value of 0,002 mm is proper (Grote and Feldhusen, 2007, p. B 49).

The local pressure loss Δp_{local} is given by:

$$\Delta p_{local} = \frac{\rho * (u^2/2)}{C_k} \quad (11)$$

Where C_k is the local loss coefficient. Local loss coefficients are given for different pipe shapes. For example, a relatively comprehensive table can be found in the ASHRAE Handbook 2009 Fundamentals of fluid flow.

In this thesis, pressure loss in the functional components $\Delta p_{components}$ is based on data from manufacturers, heat exchanger design or filter calculations.

2.3.2 Computational fluid dynamics

A cooperation of physicists, mathematicians and computer specialists has produced various effective tools for modern engineer. One outcome is computational fluid dynamics based on a finite element method (FEM) that can be used to calculate multiphysical phenomena. Typically, FEM is used for strength calculations of mechanical constructions where a reliable result is achieved even in a long term stress calculation. Other common applications are simulations of dynamic mechanisms, heat transfers, fluid dynamics and vibrations. FEM applied to fluid dynamics, is called computational fluid dynamics (CFD). In this thesis CFD is used to obtain a competitive reference for the empirical pressure loss calculations.

The CFD-modeling of the fluid behavior is based on the Navier-Stokes equations, which describe physical situation precisely, unfortunately the mathematical solution is insufficient. Briefly, the Navier-Stokes equations are based on the principles of mass, momentum, moment of inertia and energy conservation. By applying these laws to every molecule of the flowing fluid, a precise model of the fluid flow is constructed. The problem with the exact calculations is that computational power is still far from a level needed to solve for the movements of every molecule. Therefore, a mesh of the fluid under inspection is generated. A mesh is a net of particles, for example the shape of a tetrahedron. These particles are

connected to each other with knots in their corners. In FEM calculations, the conditions of these knots are calculated.

For an incompressible flow, the Navier-Stokes equations in the Cartesian coordinate system are given by (White, 2003, p. 228):

$$\begin{aligned} \rho g_x - \frac{\partial p}{\partial x} + \mu * \left(\frac{\partial^2 *u}{\partial *x^2} + \frac{\partial^2 *u}{\partial *y^2} + \frac{\partial^2 *u}{\partial *z^2} \right) &= \rho \frac{du}{dt} \\ \rho g_y - \frac{\partial p}{\partial y} + \mu * \left(\frac{\partial^2 *v}{\partial *x^2} + \frac{\partial^2 *v}{\partial *y^2} + \frac{\partial^2 *v}{\partial *z^2} \right) &= \rho \frac{dv}{dt} \\ \rho g_z - \frac{\partial p}{\partial z} + \mu * \left(\frac{\partial^2 *w}{\partial *x^2} + \frac{\partial^2 *w}{\partial *y^2} + \frac{\partial^2 *w}{\partial *z^2} \right) &= \rho \frac{dw}{dt} \end{aligned} \quad (12)$$

Where g_x, g_y and g_z stand for orientation of gravity, x, y and z are positions in the coordinate system, u, v and w are the velocities for x, y and z directions and t is time. Additionally, in the Navier-Stokes equations, the state of the turbulent fluid flow is in constant change as a function of time. Therefore, in the CFD calculations, a so-called averaged steady state condition for the turbulent flow is calculated (Hämäläinen and Järvinen, 2006, p. 37).

With a laminar flow, satisfying results are achieved by applying a reasonably tight mesh, which allow precise result at acceptable computational times. However, when modeling a turbulent flow, a number of knots in the mesh should be at least Re^3 (Hämäläinen and Järvinen, 2006, p. 37). The Reynolds number is often hundreds of thousands and the computational capacity is exceeded. Therefore, various models to describe turbulent flow are developed. One model is, so called the k - ε -model, where the turbulence prediction is based on kinematic energy k and kinematic dissipation ε . The standard and rather coarse k - ε -model has long been the only known turbulent model and it is still the most common (Siikonen, 2010, pp. 153-155). Despite that, results are debatable and the model contains several disadvantages. When using the k - ε -model, it is important to have a precise boundary layer of the mesh next to the walls where most of the turbulence is occurring (Hämäläinen and Järvinen, 2006, pp. 40-42).

In addition to the mesh definitions, the user also has to set up also boundary conditions, which are properties for inlet and outlet air and walls. Known conditions such as mean velocity, pressure, kinematic energy and kinematic dissi-

pation of the inlet air should be given and outlet conditions under calculation should be left open. Boundary conditions can be based on experimental data or calculated estimations. However, boundary conditions will never match with reality (Hämäläinen and Järvinen, 2006, pp. 40-42). After the mesh and boundary conditions are set, various iterative solving methods are applied. The result is calculated by a so-called solver which calculates until a user-specified convergence tolerance of the result is reached. Finally, results are analyzed with a post processor which creates graphical models of the calculated result.

In this thesis COMSOL Multiphysics 4.0a is used for CFD. The user-friendly interface of the COMSOL guides user rather far with CFD settings. Therefore, settings for the mesh, solver and wall conditions are automatically optimized. The inlet and outlet conditions, including the kinematic energy and dissipation are calculated by hand.

2.4 Fans

In ventilation systems, fans, also known as blowers are used to transfer air through the room which is to be ventilated. To ensure proper ventilation and inside pressure conditions, at least two fans are needed to drive the supply air and exhaust air flows, which are nearly equal in the magnitude of volumetric flow. Every fan in the system has to compensate for the static pressure loss caused by the air ducts, house and functional components inside the ventilation device. Fan types are divided into main groups according to the shape of the impeller and working method: axial fans, radial fans and tangential blowers (2008 ASHRAE handbook, 2008, pp. 20.1-20.2). In this thesis the efficiency of fans is crucial as they are main electric consumers.

With axial fans, the direction of the air flow is parallel to the rotating axis of the propel. The efficiency of the axial fan is relatively high in a free flow system but decreases dramatically in pressured systems. Tangential blowers can transfer high volumetric flows compared to the physical size of the fan and create rather high pressures, but its efficiency is significantly lower in comparison to the other fan types. Radial fans (centrifugal fans) can produce rather high differ-

ential pressures at small volumetric flows with a high efficiency, therefore radial fans are used in the detached house ventilation (2008 ASHRAE handbook, 2008, p. 20.2).

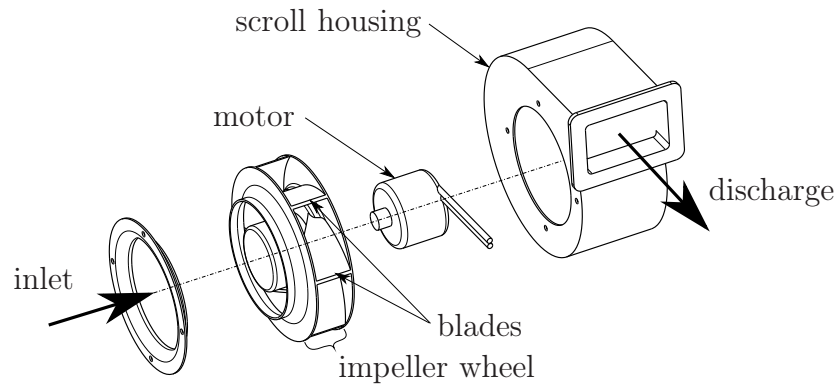


FIGURE 13. Structure of centrifugal fan (according to 2008 ASHRAE handbook, 2008, p. 20.1).

In Figure 13, functional parts of a centrifugal fan are shown. The air flow of the centrifugal fan is generated by a rotating impeller wheel which transfers kinetic and static energy to the air. In operation, the impeller wheel is rotating and centrifugal force is pushing the air columns between the impeller blades to the radial direction. When air is leaving from the impeller, the blades are adding tangential velocity to the air. Therefore, as a result the speed and direction of the air flow is a combination of the radial and tangential components. This increase in the velocity of the discharging air causes suction to the inlet and pressure to the outlet. To maximize efficiency, both velocity components of the discharged air are necessary to exploit. Hence, often a housing shape of scroll is used (2008 ASHRAE handbook, 2008, p. 20.2).

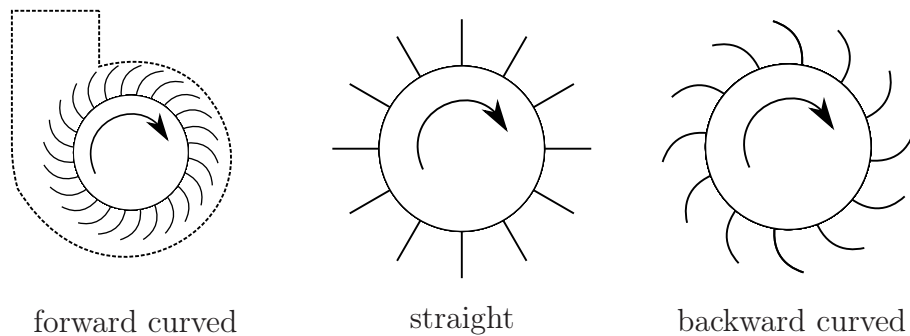


FIGURE 14. Shapes of impeller blades (according to 2008 ASHRAE handbook, 2008, p. 20.2).

Centrifugal fans are classified to the forward curved, backward curved and straight blade fan types according to the contour of the impeller blades (see Figure 14). In the forward curved fan type, blades of the impeller are bent to the direction of rotation. In general, the number of blades is higher than in other variants, thus the size of the impeller is significantly smaller. Nonetheless, to create an air flow with a forward curved fan, the scroll housing is necessary. Consequently, the size is equal with the other variants. In regards to the numerous blades, a pressure shock caused by each blade is smaller. Consequently the forward curved fan type is the most silent centrifugal fan type. The volumetric flow created by a forward curved fan is nearly independent from the increase of the pressure resistance in system caused by the dirt accumulation in filters. That allows a simple fan control and easy maintenance. Hence, the forward curved fan type is the most often used fan in domestic ventilation. The disadvantage of the forward curved fan type is a low efficiency of only up to 60 % (2008 ASHRAE handbook, 2008, p. 20.2).

A straight bladed fan type is designed for dirty air and its efficiency is extremely low only up to 50 %. Thus, the use of the straight bladed fan type is insensible in domestic ventilation systems. By curving the blades of the impeller backwards, sensibility for dirt increases, but also a relatively high efficiency of up to 80 % is reached (2008 ASHRAE handbook, 2008, p. 20.2). The main reason why the efficient backward curved fans are not in common domestic use is due to the rather high noise caused by the pressure shocks from very few impeller blades. In addition to that, the volumetric flow is related to the pressure and additional sensors to control the fan are necessary. However, because of its high efficiency, the backward curved fan type has to taken account in the DEC system.

TABLE 1. Fan laws (according to 2008 ASHRAE handbook, 2008, p. 20.4).

Law No.	Known	
1a	n_1	$Q_1 = Q_2 * \left(\frac{D_{fan1}}{D_{fan2}}\right)^3 * \frac{n_2}{n_1}$
1b		$p_1 = p_2 * \left(\frac{D_{fan1}}{D_{fan2}}\right)^2 * \left(\frac{n_2}{n_1}\right)^2 * \frac{\rho_1}{\rho_2}$
1c		$P_1 = P_2 * \left(\frac{D_{fan1}}{D_{fan2}}\right)^5 * \left(\frac{n_2}{n_1}\right)^3 * \frac{\rho_1}{\rho_2}$
2a	p_1	$Q_1 = Q_2 * \left(\frac{D_{fan1}}{D_{fan2}}\right)^2 * \sqrt{\frac{p_1}{p_2}} * \sqrt{\frac{\rho_2}{\rho_1}}$
2b		$n_1 = n_2 * \frac{D_{fan2}}{D_{fan1}} * \sqrt{\frac{p_1}{p_2}} * \sqrt{\frac{\rho_2}{\rho_1}}$
2c		$P_1 = P_2 * \left(\frac{D_{fan1}}{D_{fan2}}\right)^2 * \left(\frac{p_1}{p_2}\right)^{\frac{3}{2}} * \sqrt{\frac{\rho_2}{\rho_1}}$
3a	Q_1	$n_1 = n_2 * \left(\frac{D_{fan2}}{D_{fan1}}\right)^3 * \frac{Q_1}{Q_2}$
3b		$p_1 = p_2 * \left(\frac{D_{fan2}}{D_{fan1}}\right)^4 * \left(\frac{Q_1}{Q_2}\right)^2 * \frac{\rho_1}{\rho_2}$
3c		$P_1 = P_2 * \left(\frac{D_{fan2}}{D_{fan1}}\right)^4 * \left(\frac{Q_1}{Q_2}\right)^3 * \frac{\rho_1}{\rho_2}$

Each fan has a fan curve which describes the characteristic performance of the fan. The fan curve is the most important source of information in the optimization of a fan application. The fan curve is based on three fan laws where the variables are volumetric flow Q , pressure p , power P , specific fan size D_{fan} , rotation speed n and density ρ (see Table 1). Subscript 1 stands for the fan operating point under inspection and subscript 2 for the values in a tested operating point of the fan. For all fan laws, mechanical efficiency of the fan η_{fan} is assumed to be constant between both points of rating (2008 ASHRAE handbook, 2008, pp. 20.4-20.5). The fan laws are good when the performance properties of a fan have to be calculated for various operating points.

An example of a fan curve graph is shown in Figure 15. The pressure increase p is shown as a function of the volumetric flow Q for different rotational speeds n . Complete efficiency curves $\eta_3 < \eta_2 < \eta_1$ are also given. The complete efficiency is a combination of the mechanical efficiency of the fan η_{fan} and efficiency of the motor η_{motor} . System curves are describing a pressure resistance of the system as a function of the volumetric flow. In an ideal situation, the fan size and type are optimized so that the operating point is always in the area of the highest effi-

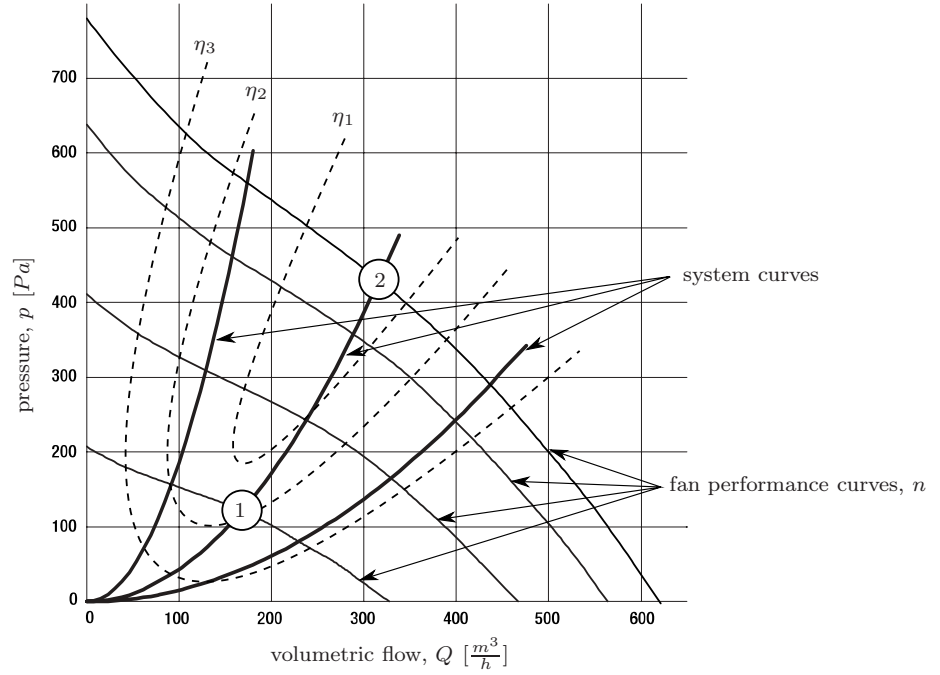


FIGURE 15. Fan curves (according to 2008 ASHRAE handbook, 2008, p. 20.5).

ciency. In practice, the situation is never ideal, because the pressure resistance of the ventilation systems increases as a function of time due to increasing amount of dirt in filters. Additionally, ventilation is driven on various volumetric flows regarding to the ventilation needs, for example day and night settings. Therefore, the fan laws and the fan curves are necessary tools, when optimizing a fan for several operating points.

A theoretical example of the use of the fan laws when efficiency, density and the specific fans size are constant follows. In Figure 15, the values of the operating point 1 at volumetric flow $Q_1 = 165 \frac{m^3}{h}$ can be calculated from the values of the tested operating point 2. In the tested point 2, the collected values are:

$$n_2 = 3630 \text{ rpm}, P_2 = 103 \text{ W}, p_2 = 430 \text{ Pa}, Q_2 = 320 \frac{m^3}{h}$$

As the Q_1 is known, according to the fan law 3b pressure p_1 is given by:

$$p_1 = p_2 * \left(\frac{Q_1}{Q_2}\right)^2 \Rightarrow p_1 \approx 114,32 \dots \text{ Pa}$$

According to the fan laws and 3c, needed power P_1 is given by:

$$P_1 = P_2 * \left(\frac{Q_1}{Q_2}\right)^3 \Rightarrow P_1 \approx 14,12 \dots \text{ W}$$

According to the fan laws and 3a, rotation speed n_1 is given by:

$$n_1 = n_2 * \frac{Q_1}{Q_2} \Rightarrow n_1 \approx 1871,71. . . rpm$$

In general, for centrifugal fans that are applied to domestic ventilation, a motor is positioned into the middle of the impeller. Thus, the motor is in direct contact to the air stream. Most of the energy loss of the fan is from the motor and occurs as temperature increases over the fan. The temperature change $\Delta\vartheta$ is given in Equation 13 where ρ_{air} is density of the air, Δp is the pressure increase, η_{fan} is the efficiency of the fan, η_{motor} is the efficiency of the motor and $c_{p,air}$ is the specific heat capacity of air (2008 ASHRAE handbook, 2008, p. 21.6).

$$\Delta\vartheta = \frac{\Delta p}{\rho_{air} * c_{p,air} * (\eta_{fan} * \eta_{motor})} \quad (13)$$

2.5 Filters

Nowadays, people spend nearly 90 % of their time indoors (Korhonen and Lintunen, 2003, p. 13). People breathe inside air continuously and through their lungs all the particles of the air affect to the body. Especially in urban areas, air is often polluted by traffic and industry. Hence, the air contains a lot of harmful particles. In addition, the air of rural areas contains living microbes from nature and agricultural operations which can cause unwanted reactions in the body. To control the inside air quality, various standards and building regulations regarding the air ventilation systems are legislated.

In air ventilation, the quality of the air is controlled by supply and exhaust air filters. Ventilation filters are divided into three groups, coarse (G), medium (M) and fine (F) by the penetration percent of unwanted molecules, in medium and fine filters particles with a diameter of $0,4 \mu m$ are under inspection (DIN EN 779, 2009, p. 14). In clean air areas, such as villages and suburbs, to ensure middle quality of the inside air for non-residential buildings, supply air has to be filtered with at least F7-class filter (DIN EN 13779, 2007, p. 44). For residential buildings, only recommendations for the supply air filters are set. These recom-

recommendations are based on research regarding to the long-term effects of bad inside air quality. In rural areas filtering level F7 and in urban areas filtering level F8 are preferred (Sisäilmastoluokitus 2008, 2008). In addition, to protect the functional components of the ventilation device from dirt and mechanical damage and to avoid unwanted particles outside, the exhaust air of the residential buildings has to be filtered with at least G2-class filter (DIN 1946-6, 2009, p. 56).

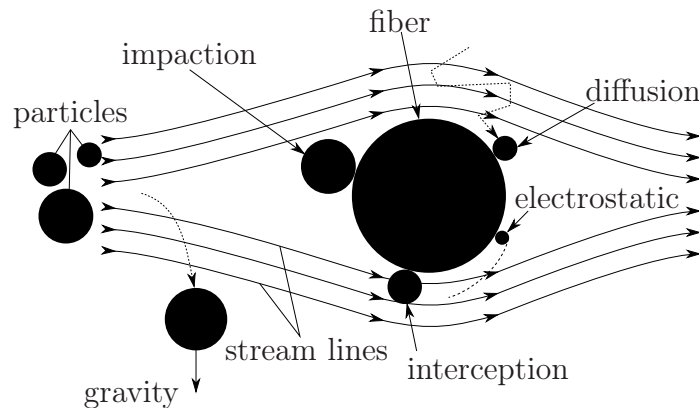


FIGURE 16. Ways of particle collection in fibrous filters (according to Ensor and Donovan, 1988, pp. 8-9).

Most of the ventilation filter elements are made of various fibers such as natural and synthetic glass fibers. In fibrous filters, filtering is based on diffusion, inertial impaction, interception, electrostatic attraction and gravity (see Figure 16). When filtering outside air suitable for a supply, the diameter of the particles is rather small, usually less than $1\ \mu m$. In the filtration of such small molecules, the main ways to collect particles are diffusion, diffusion-interception and interception (Ensor and Donovan, 1988, pp. 8-9). According to the filter testing procedure, only mechanical ways of filtering are counted and the effect of the electrostatics is excluded (DIN EN 779, 2009, p. 6).

According to this physical background and the exclusion of electrostatic attraction, the efficiency and pressure drop in fibrous filters can be predicted relatively precisely. The prediction is based on the filtering efficiency of a single fiber in the filter element. For a single fiber efficiency of diffusion, diffusion-interception and interception are conducted from physical values of unwanted particles and used fibers. After the efficiency of a single fiber is known, the structure for the whole filter element is defined according to required efficiency. By combining

values of passing flow and structure of filter element, the pressure drop is given (Davies, 1952, pp. 185-198):

$$\Delta p = \frac{u_{facing} * Z_{filter} * \mu}{d_{fiber}} * [64 * \alpha_{filter}^{1.5} * (1 - 56 * \alpha_{filter}^3)] \quad (14)$$

In this formula, the pressure drop Δp is defined by the solidity of the air a filter element α_{filter} , the average diameter of the single fiber d_{fiber} , the thickness of the filter Z_{filter} , the mean facing velocity between the passing fluid and the filter u_{facing} and the dynamic viscosity of the passing fluid μ . Formulas to calculate the filter efficiency and the graph for the pressure drop in standard filters is given in Appendix 10.

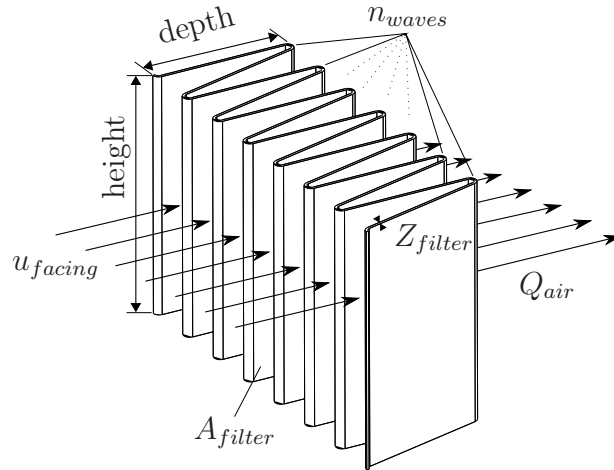


FIGURE 17. Factors of filter design.

Normally, standard filters as shown in Figure 17 are positioned into filter elements. By waving the filter cloth, a surface area A_{filter} increases and facing velocity u_{facing} of the air flow Q_{air} decreases, thereby the pressure drop is reduced. Z_{filter} is a thickness of the filter cloth, which is related to efficiency and pressure drop. The facing velocity is given in Equation 15, where is n_{waves} is the number of the waves, h is height and d is depth.

$$u_{facing} = \frac{Q_{air}}{h * d * n_{waves} * 2} \quad (15)$$

2.6 Water hydraulics

A device which moves a liquid from one place to another is called a pump. In many cases, a liquid is also transferred from a lower level to a higher level. According to the structures and working mechanisms of the pumps, pump types are divided into the hydrostatic and hydrodynamic pumps. In the hydrodynamic pump type the inlet and the outlet sides are connected. Therefore, a volumetric flow is dependent on the current system pressure resistance. In the hydrostatic pump type, such as a piston pump and a gear pump, the inlet and the outlet side are separated with valves, sealings or gear teeth, thus the volumetric flow is assumed constant.

A centrifugal pump is a hydrodynamic pump and covers 80 % of the pumping demand in the process industry. The centrifugal pump is widely used, because it is suitable for various applications, when low viscosity fluids have to be transferred (Luukkanen, 2001, p. 11). In addition, a smooth hydrodynamic behavior and a simple structure ensure a long lifetime and easy maintenance. Generally, in low pressure water applications such as the DEC water cycles in this thesis, a centrifugal pump is the most sensible.

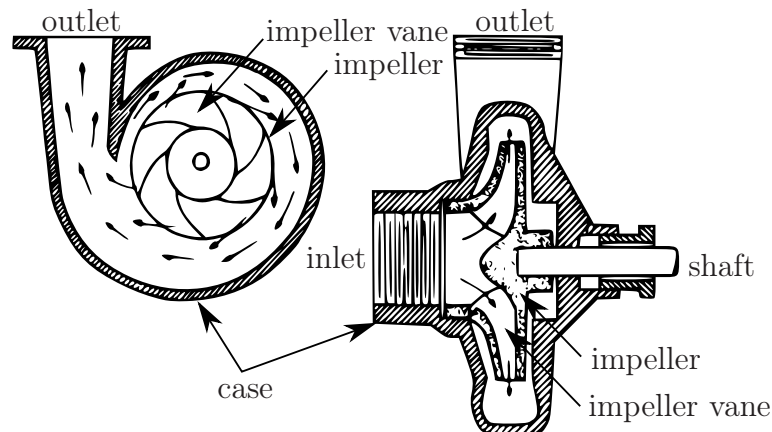


FIGURE 18. Functional parts of centrifugal pump (according to 2008 ASHRAE handbook, 2008, p. 43.2).

A centrifugal pump consists of only a few functional parts, shown in Figure 18. The inlet and outlet pipes are connected to the case, which is the main body of the pump. Inside and in the middle of the case is the impeller. The impeller is rotated by the motor which is connected to the shaft. The impeller consists of several impeller vanes which create the actual volumetric flow. When the im-

PELLER IS ROTATING, THE OUTSIDE CURVED IMPELLER VANES ARE FORCING THE LIQUID INTO A RADICAL MOVEMENT. THE LIQUID EXPERIENCES COLLISION TO THE CASE AND STARTS MOVING TOWARDS THE OUTLET. IN THE COLLISION, PART OF THE KINETIC ENERGY CHANGES TO THE PRESSURE. IN A CONTINUOUS ROTATION, THE DESIRED PRESSURE DIFFERENCE BETWEEN THE INLET AND THE OUTLET OCCURS. DURING THE PUMPING THE INLET, THE OUTLET, THE IMPELLER VANES, AND THE WHOLE CASE ARE FULL OF LIQUID (2008 ASHRAE HANDBOOK, 2008, pp. 43.1-43.2).

IN PUMP OPTIMIZATION, PERFORMANCE CALCULATIONS ARE NEEDED. PRESSURE PERFORMANCE OF THE PUMP IS NORMALLY GIVEN IN A COMPLETE DELIVERY HEIGHT $H_{complete}$. THE PUMP CALCULATIONS ARE BASED ON THE BERNOULLI'S PRINCIPLES, WHICH DEFINE THAT THE COMPLETE DELIVERY HEIGHT IS A COMBINATION OF THE HYDROSTATIC DELIVERY HEIGHT H_{static} AND THE HYDRODYNAMIC DELIVERY HEIGHT $H_{dynamic}$. THE HYDROSTATIC DELIVERY HEIGHT IS THE COMBINATION OF THE ACTUAL DELIVERY HEIGHT DIFFERENCE BETWEEN THE INITIAL LEVEL h_i AND THE END LEVEL h_e , AND THE ADDITIONAL PRESSURE DIFFERENCE BETWEEN THE SURROUNDING AIR PRESSURE $p_{surrounding}$ AND THE PRESSURE OF THE TANK p_{tank} . HYDRODYNAMIC DELIVERY HEIGHT IS CONDUCTED FROM THE VELOCITY DIFFERENCE BETWEEN THE INITIAL VELOCITY u_i AND END VELOCITY u_e , AND THE PRESSURE LOSS CAUSED BY COMPONENTS $\Delta p_{components}$. IN ADDITION TO THE PRESSURE, ANOTHER IMPORTANT VALUE IS THE VOLUMETRIC FLOW Q . THE TOTAL POWER CONSUMPTION P_{total} IS RELATED FROM THE PREVIOUS VALUES AND THE EFFICIENCY OF THE PUMP UNIT η_{pump} (LUUKKANEN, 2001, P. 23).

Complete delivery height:

$$H_{complete} = H_{static} + H_{dynamic} \quad (16)$$

Hydrostatic pressure:

$$H_{static} = h_e - h_i + \frac{p_i - p_e}{\rho * g} \quad (17)$$

Hydrodynamic height:

$$H_{dynamic} = \frac{u_e^2 - u_i^2}{2 * g} + \frac{\Delta p_{components}}{\rho * g} \quad (18)$$

Hydraulic power:

$$P_{hydraulic} = H_{complete} * Q * g * \rho \quad (19)$$

Total power consumption:

$$P_{total} = \frac{P_{hydraulic}}{\eta_{pump} * \eta_{motor}} \quad (20)$$

3 DESIGN PROCESS

In this chapter, the actual design process is reported. The chapter is divided into three main stages of design, in the same order that the actual design work proceeded. Design starts with the setting of requirements and several estimations which are needed to have initial data to start the design. In doing selections of the components, and creating ideas of the structure, more facts are justified and estimations become more precise. Thereafter, the main components and important design factors of them are determined. The chapter ends to the point where competence of the DEC process can be proven.

3.1 First stage

In the first stage of the design, product requirements are discussed. Then, the design work itself is started with the efficiency estimations based on the theoretical setup of the DEC system. These estimations will stay in the background during the whole design, and will be defined step by step more precisely. The first step closer to the actual construction, is a new solution to change the adsorption and desorption phases only with one active valve. The first construction based on the new valve mechanism is shown but many open questions have to be cleared up in the next steps.

3.1.1 Requirement list and objectives

The product development is started with the requirement list and the project objectives, see Appendix 1. The project requirements are written out with respect to the top project requirements and to the nature of the DEC process. In general, only the required cooling performance, its intended use in detached house applications and basic functions of the DEC system are fixed. The rest of the points in the requirement list are carried out from these main requirements with respect to the principles of the machine building and the general defini-

tions of the ventilation units. Above all the requirements, the main intention is to prove the competitiveness of the actual product.

Objectives for this thesis are written out according to the early state of the product development. Regarding to that, the desired design results include conceptual 3D models, general part lists, efficiency calculations, comparison between different solutions, and a clearance of the competence or incompetence of the product.

3.1.2 Efficiency estimations

The most important step of the whole development process is to determine if it is possible to reach all the critical requirements. Although, the competence of the DEC process is proved in a larger scale and in the testing lab of CR/AEB, the electric cooling coefficient of performance $COP_{electric}$ of 20 appears difficult to meet. In addition, it is important to clarify several power consumptions and efficiencies for such a multiple power source system.

To determine the possibilities regarding to the electric cooling efficiency, rough estimations of a power consumption are shown in Appendix 4. The power consumption is allocated to the power consumption of a standard ventilation $P_{standard}$ and the additional electric power to drive cooling process $P_{cooling}$. The standard ventilation means a standard air handling in residential buildings, which is running constantly to ensure the inside air quality. $P_{cooling}$ contains all the additional power consumption in comparison to the standard ventilation which is needed during the cooling process to reach the desired thermal cooling power P_{cold} of 3,3 kW. Thus, the complete electric power consumption consists of the standard and the cooling process power consumption and is given by:

$$P_{complete} = P_{standard} + P_{cooling} \quad (21)$$

The electric power consumption of a standard ventilation system is classified into the pressure loss (air handling components) and electricity (control unit).

Nonetheless, the pressure loss is compensated with electrically driven fans. In the cooling process more components, an additional solar thermal power source, water circulations and a higher volumetric flow of the air are needed. When estimating the electric cooling coefficient of performance $COP_{electric}$, the solar thermal power P_{solar} used for the regeneration of silica gel, is assumed to be free. In addition, a part of the standard ventilation $P_{standard}$ is excluded because it is needed in every residential room. Therefore, to meet the $COP_{electric}$ requirement of the cooling, all additional electric power in the cooling mode $P_{electric}$ which is needed in the cooling process to compensate additional pressure loss and to drive water circulation is given by (based on Henning, 2004, pp. 15-16):

$$COP_{electric} = \frac{P_{cold}}{P_{complete} - P_{standard} - P_{solar}} = \frac{P_{cold}}{P_{cooling} - P_{solar}} = \frac{3,3kW}{P_{electric}} \geq 20 \quad (22)$$

$$\begin{aligned} \Rightarrow P_{electric} &\geq 165W \\ &\Rightarrow \textit{requirement} \end{aligned} \quad (23)$$

In addition to that, it is planned to be use the device approximately 75 % of the time on the standard ventilation in the winter mode. Hence, it is important to meet high efficiency also during the standard ventilation. To stay in a neutral range, competitor products on the market can be used as a baseline (see Appendix 6). According to these products, the power consumption at volumetric flow of 175 - 210 $\frac{m^3}{h}$ with heat recovery should be approximately 60 - 95 W.

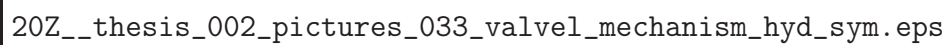
After an initial research, it becomes clear that main electric consumption in the cooling process is created by the fans. In the cooling mode a supply fan (Fan 1), exhaust fan (Fan 2) and desorption fan (Fan 3) are used to drive the system properly. These fans are each creating a volumetric flow of 350 $\frac{m^3}{h}$ through the house and the desorption process. The fans are compensating the pressure loss of various components. In Appendix 4, the initially estimated pressure losses for each fan are shown. Supply fan has to compensate $\approx 325 Pa$, exhaust fan $\approx 285 Pa$ and desorption fan $\approx 120 Pa$. The pressure drop assumed in coated

heat exchangers is based on prototype measurements and the IEC values are based on supplier data and experimental tests in the lab. The rest of the values are rough estimations.

In Appendix 5, three fan setups to compensate the estimated pressure loss at the required volumetric flow are shown. All the fans used are produced by ebmpapst which is the leading supplier of the energy saving fans used in ventilation systems. Fan setups under consideration are powered by direct current (DC), as DC fans consume up to 30 % less energy than alternate current (AC) powered fans (Weinmann, 2011). In the first setup, similar forward curved fans compared to the competitor products are used, but the efficiency reached is not enough ($COP_{electric} \approx 14$). In the second setup bigger forward curved fans are used and the efficiency is better ($COP_{electric} \approx 19$), but still does not meet with requirements. In the third setup high efficient backward curved fans are applied and high electric cooling coefficient of performance can be reached ($COP_{electric} \approx 24$). As a result from the initial efficiency estimations, the DEC process is possible to realize with the desired $COP_{electric}$.

3.1.3 Valve mechanism to control air flows

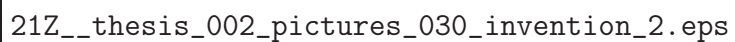
[Text deleted due to confidentiality]



20Z__thesis_002_pictures_033_valvel_mechanism_hyd_sym.eps

FIGURE 19. Symbol of required valve.

[Text deleted due to confidentiality]



21Z__thesis_002_pictures_030_invention_2.eps

FIGURE 20. Principles of the valve mechanism.

[Text deleted due to confidentiality]

[Text deleted due to confidentiality]

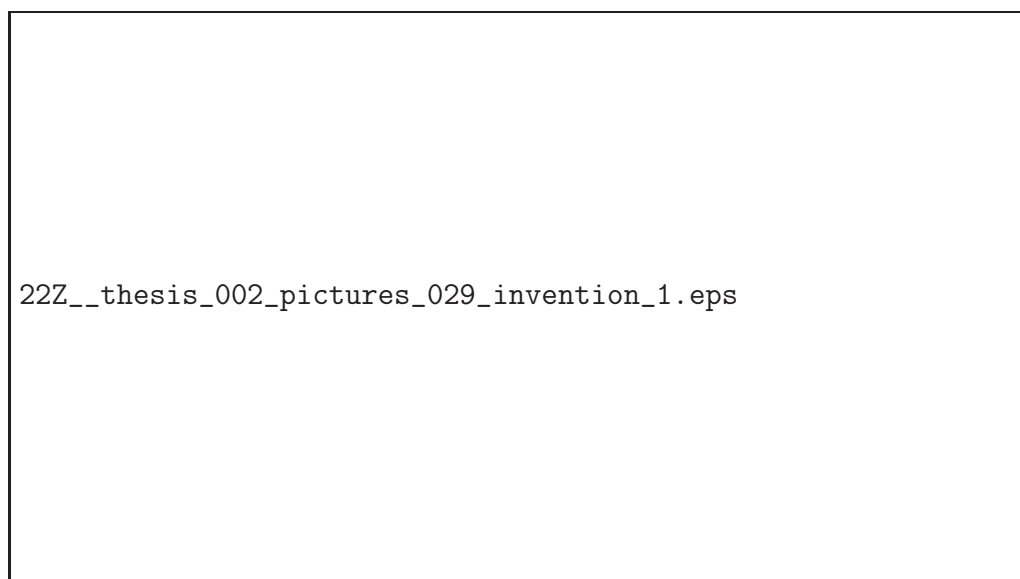
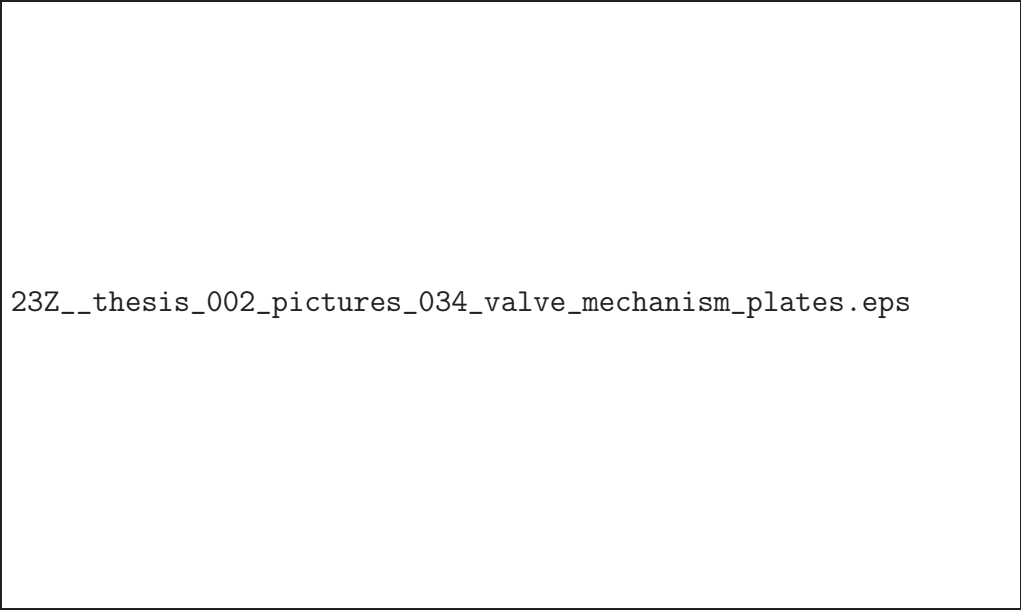


FIGURE 21. Back and front view of valve mechanism.

[Text deleted due to confidentiality]

[Text deleted due to confidentiality]



23Z__thesis_002_pictures_034_valve_mechanism_plates.eps

FIGURE 22. Sheet metal plates.

[Text deleted due to confidentiality]



24Z__thesis_002_pictures_035_passive_valve.eps

FIGURE 23. Fan box and back flow valve.

[Text deleted due to confidentiality]

3.1.4 First construction

[Text deleted due to confidentiality]



FIGURE 24. First construction.

[Text deleted due to confidentiality]

[Text deleted due to confidentiality]

[Text deleted due to confidentiality]

3.2 Second stage

[Text deleted due to confidentiality]

3.2.1 Fan design

Now the implementation of the fans is discussed. As derived in Section 2.4 it is favorable to use backward curved fans in proper housings. Fan design is done due to a new generation of the backward curved EC powered fans from the fan supplier ebm-papst. The newest fan generation is called RadiCal. The impeller wheel of the RadiCal fan is shown in Figure 25. The impeller wheel of the RadiCal fan is based on new fiber composite manufacturing methods. Therefore, new solutions from CFD research of the impeller geometry are possible to apply. Consequently, the impeller wheel contains several advantages in comparison to the old generations. The rounded contour of the base and cover plates increase the efficiency. In addition, a new inlet flange (not shown in figure) creates more effective suction. A new styling of the air flow channels between the blades generates continuous flow and reduces significantly the amplitude of the pressure shocks. Regarding pressure shock reduction, a noise level is reduced by 8 *dB* in the considered operation points of the DEC system (Weinmann, 2011).

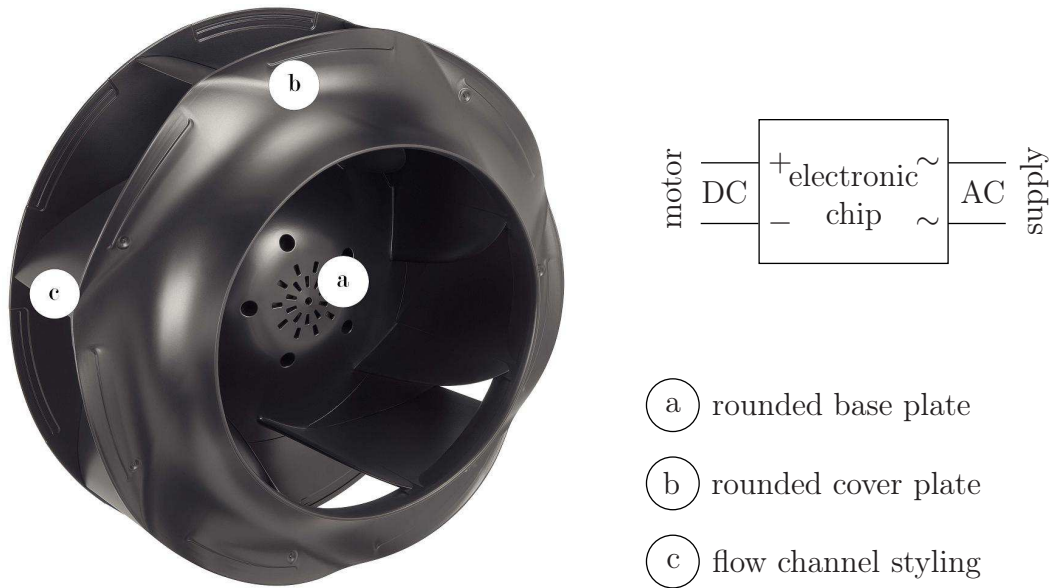


FIGURE 25. RadiCal fan and EC power.

In addition, a new motor technology (called GreenTech EC motors), can be applied. Motors are EC powered, which means that AC is converted to DC by a specialized high efficient electronic chip (see Figure 25). The electronic chip is mounted directly to the motor unit and substitutes all electronics that are necessary to power standard DC and AC motors. Hence, the size of the motor is smaller. With the EC technology an efficiency of motor up to 80 % can be reached. In comparison to ordinary DC powered fans, power consumption is 15 % less, and compared to the AC powered fans 50 % less. Furthermore, the EC powered motors are relatively silent (Weinmann, 2011). In Appendix 7 a comparison of the power consumption and the noise level between the RadiCal, old generation, and the forward curved fan types is shown in estimated operating points which are clarified in Appendix 4.

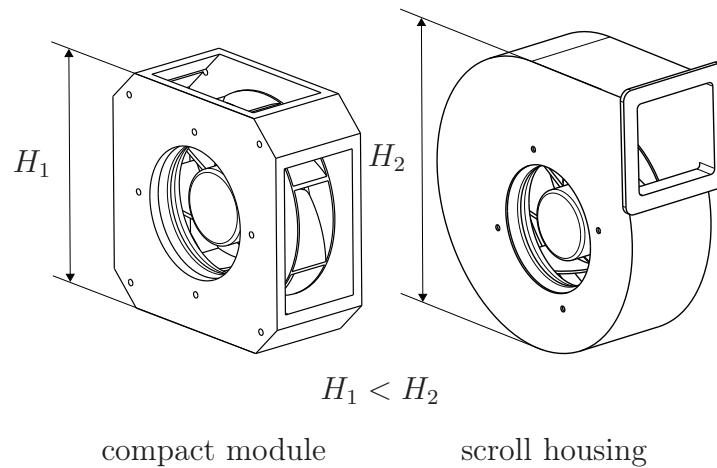


FIGURE 26. Compact module and scroll housing.

Apart from the application of the new fan technologies, the positioning of backward curved fans has a significant impact on the efficiency. According to information from ebm-papst, two ways are commonly used to implement the fans: compact fan modules or design the scroll housing. Compact modules are smaller in height compared to ordinary scroll housing (see Figure 26). In addition, the more rectangular shape of the compact module is easier to apply than the round shaped scroll housing. To reach the highest possible efficiency, at least 180° around the module should be open. By doing self designed scroll housing, efficiency can be significantly higher compared to scroll housing, but the size of the fan unit is increasing. In further design the advantages of compact fan housing have to be inspected, otherwise the scroll housing is the most sensible solution (Weinmann, 2011).

In Appendix 7, the calculation of the achieved efficiency with RadiCal fans is calculated. According to this calculation, the $COP_{electric}$ is increased even up to 26,6 which is 2,4 units more compared to the first backward curved fan setup. The difference seems relatively small, but it is important to notice that the standard power consumption decreases from 54 W to 42 W which partly reduces the $COP_{electric}$. As a result from the application of new generation the reached $COP_{electric}$ is even higher than required in the specifications.

3.2.2 Applying indirect evaporative cooling to the cooling box

[Text deleted due to confidentiality]

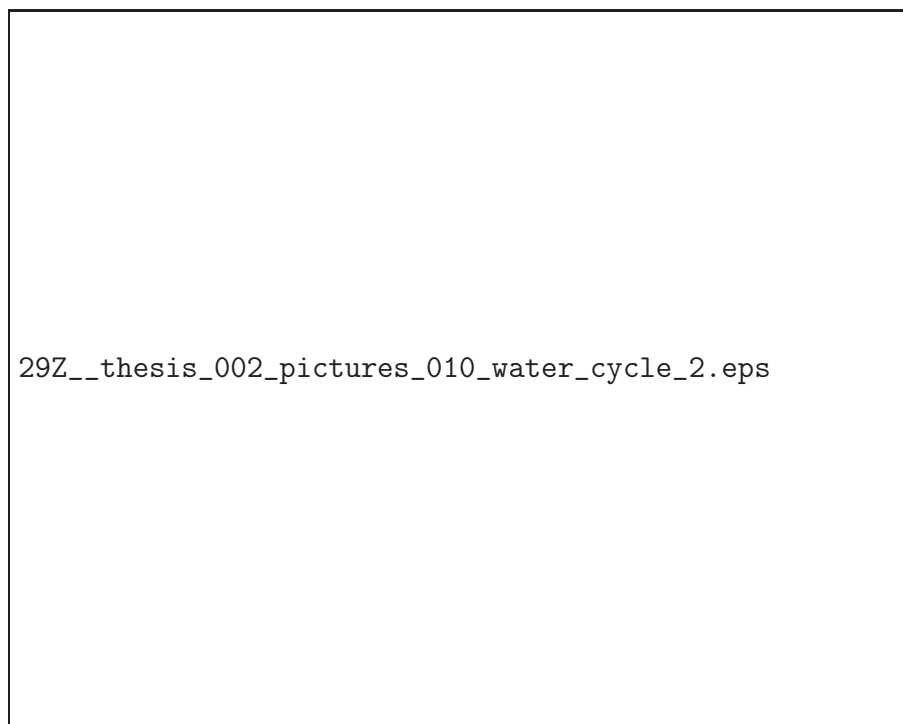


FIGURE 27. Direct and indirect cooling box.

[Text deleted due to confidentiality]

[Text deleted due to confidentiality]

3.2.3 Second construction

[Text deleted due to confidentiality]



FIGURE 28. Second construction.

[Text deleted due to confidentiality]

[Text deleted due to confidentiality]

[Text deleted due to confidentiality]

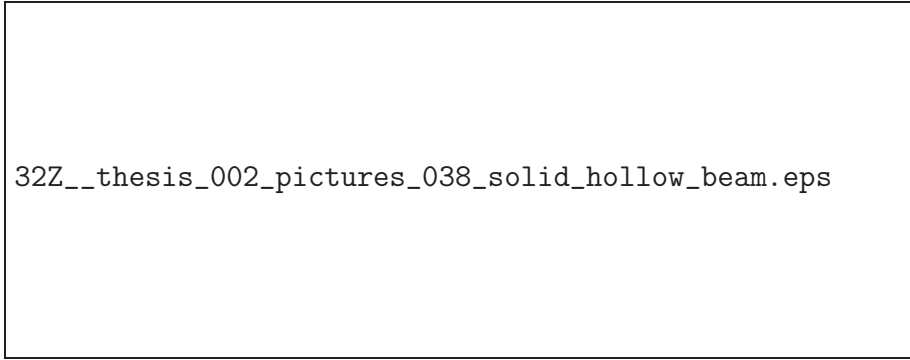
3.2.4 Optimization of valve mechanism

[Text deleted due to confidentiality]



FIGURE 29. Valve mechanism driven by electric cylinder.

[Text deleted due to confidentiality]



32Z__thesis_002_pictures_038_solid_hollow_beam.eps

FIGURE 30. Solid and hollow beam.

[Text deleted due to confidentiality]

[Text deleted due to confidentiality]

3.3 Third stage

The third and final stage is to apply the rest of the needed components into the construction. First, the filter elements are fitted into the structure and the pressure loss in them is calculated. After that, the required water cycles are designed and the power consumption during the cooling operation is explained. Then, a third and final construction is shown, where all components of the design are applied in optimized fashion. When all the components have their fixed position and sizes, a comprehensive pressure loss calculation can be conducted. The pressure loss in the structure is calculated in an empirical and numerical way as discussed in Sections 2.3.1 and 2.3.2. According to the result, the operating points for the fans in terms of volumetric flow and pressure loss are known. Furthermore, the total $COP_{electric}$ is defined, and the competence of the DEC system in a detached house use is proven.

3.3.1 Filters

To ensure a high quality ventilation and to meet with the standards as given in Section 2.5, the decision is to use F7 class supply air filtration and G3 class exhaust air filtration. To extend the changing time of the supply air filters, pre-filtering with a coarse filter type G3 is preferred in front of the fine filter. According to the first and second construction, several supply air filters are needed. Separate G3 and F7 class filters are needed for both coated heat exchangers and for the bypass valve used in the winter mode. Additionally, a G3 class exhaust filter to clear the discharged air has to be positioned before the water spray into the cross counter flow heat exchanger. A G3 class filter for the desorption air can be positioned directly after the desorption fan.



FIGURE 31. Filter setup.

Generally, the use of fibrous filters is preferred, as the efficiency is high compared to the price. However, the high efficiency cuts the lifetime and filters have to be changed twice a year. In the filter setup (see Figure 31), supply and desorption air is driven through two separated G3 and F7 class filters in summer mode, and in winter mode through another set of G3 and F7 class filters. According to this alternating use of filters, one change a year is sufficient. Due to the equal life time wanted between coarse and fine filters, the surface area of filters is preferred to be equal.

In the first and second construction no space is reserved for the filters. The intake filters have to be positioned in front of the coated heat exchangers and the most logical way is to install filters as shown in Figure 31. The available space in the front of the coated heat exchangers is unacceptably small in the earlier constructions and therefore new dimensions have to be set. Space for the filters is created by reducing the intake distribution space, shortening the coated heat exchangers, reducing the size of the valve mechanism and the supply air channel in front of the device. The dimensions for the filters are shown in Figure 32. The exhaust filter for the discharged air is positioned before the water spraying and



FIGURE 32. Size optimization for filters.

TABLE 2. Pressure drop in filter elements.

Air flow	Filter	Q_{air} [m^3/h]	height [mm]	depth [mm]	n_{waves}	u_{facing} [m/s]	Δp [Pa]
Supply/Desorption	F7	350	400	100	20	0,06	40
Supply/Desorption	G3	350	400	100	20	0,06	5
Exhaust	G3	350	200	200	25	0,05	4
Desorption	G3	350	200	200	20	0,06	5
Bypass	F7	175	400	100	20	0,03	15
Bypass	G3	175	400	100	20	0,03	2,5

the exact position will be shown in the third construction (see Section 3.3.3).

Due to these changes in dimensions, the filters shown in Table 2 can be applied with respect to the pressure drop requirements. Calculations are based on Section 2.5 and Appendix 10.

3.3.2 Water cycles

[Text deleted due to confidentiality]

[Text deleted due to confidentiality]

According to the needs of the water cycles, a centrifugal pump type can be applied. For example, Grundfos AB offers water circulation pumps for domestic applications. Pumps from the series ALPHA2 have energy classification A and can electronically adjust themselves to the pumping demand. The ALPHA2 series is optimized for high volumetric flows of domestic water systems, and therefore the impeller wheel is over-sized for the DEC application. However, in the optimal point of the ALPHA2 series, the combined efficiency of the pump and the motor is 0,35-0,40 (Grundfos ALPHA2, nd). With this efficiency assumed, the calculations are shown in Appendix 11. Then, the conducted overall electric pumping power required is approximately 28 *W*.

3.3.3 Third construction

[Text deleted due to confidentiality]



FIGURE 33. Third construction.

[Text deleted due to confidentiality]

[Text deleted due to confidentiality]

3.3.4 Pressure loss and power consumption

Finally, when all the required components are positioned in the third construction, the pressure loss in the complete system can be calculated. The pressure loss for the structure is calculated by the empirical and numerical method (see Appendix 13 and 14). In order to apply the empirical method, the structure is simplified and many assumptions are made. First, all the hydraulic dimensions of supply, exhaust and desorption flows are measured from built 3D models. According to the measured values and hydraulic diameters, the mean velocities of the air are calculated. Then, the given equations are applied and friction loss in all channels and local losses in corners are calculated.

The empirical method is deemed valid only for a fully developed flow. In the ventilation devices, the flow is never fully developed and therefore the values from the empirical method are cross-checked with results calculated by using the CFD. For this method the models used are simplified. For example, all the components are empty channels and rounded structures are disabled. The pressure drop due to the components is added to the pressure drop due to the structure. To reach nearly realistic boundary conditions for inlet and outlet flow, all ducts are lengthened to 400 *mm*.

As a result from the pressure loss calculations, during the cooling process, the effect of the structure itself can be stated relatively small $\approx 50 Pa$ in comparison to other components $\approx 577 Pa$. Furthermore, the difference between the empirical and numerical methods is negligible in a low pressure system such as an air ventilation device. Hence, the empirical method can be used for further optimization.

Due to the pressure loss calculations (see Appendix 13 and 14), the power consumption of RadiCal fans during the cooling process and standard ventilation can be calculated more precisely.

TABLE 3. The total power consumption of the fans.

Fan	$\Delta p [Pa]$	$Q [m^3/h]$		$P [W]$
Cooling process				
Supply fan	279	350	\Rightarrow	56
Exhaust fan	253	350	\Rightarrow	52
Desorption fan	89	350	\Rightarrow	20
Total				128
Standard ventilation				
Supply fan	182	175	\Rightarrow	22
Exhaust fan	175	175	\Rightarrow	20
Total				42

To get the overall electric consumption, the consumption of fans and the power consumption of water cycles are taken into account. As a result, the total $COP_{electric}$ can be calculated (see Table 4). The reached electric cooling coefficient of performance is fairly in the given requirements.

TABLE 4. The total electric cooling efficiency.

	Cooling process $P_{complete} - P_{solar}$	Standard ventilation $P_{standard}$	Cooling power P_{cold}
Fans	128 W	42 W	
Water	28 W		
Total	156 W	42 W	3300 W
$\Rightarrow COP_{electric} \approx 28,95\dots$			

In addition to the electric cooling efficiency, the temperature increase over the fan has to be determined. In fact, the supply fan consumes 56 W which will in the end occur completely as a temperature increase in the resisting components, ducts and house. Nonetheless, the process values discussed in the Section 2.2.2 are based on the experimental data where the effect of the components is already compensated. Due to that, only the temperature increase over the supply fan is clarified. The temperature increase is approximately 0,30 K and can be deemed insignificant.

4 CONCLUSION

During the design process, the path to the results was not as straightforward as it was assumed in the beginning. Regarding to the lack of the DEC and the ventilation device design guidelines, it was necessary to conduct a comprehensive research into the theory and the fundamentals of every component. The component variety in such a device is rather wide and the fundamentals are multi-physical, thus the theory part is quite extensive. For example, after an initial research of filters, the design material from the filter manufacturers was realized inadequate, and the decision was to carry out the whole design from a single fiber to the complete element. Compared to the mechanical fundamentals, air conditioning is highly legislated and regulated, thus the standards and regulations had to be clarified.

In the beginning, a detached house application with the necessary DEC components was nearly impossible to fit to the required size. This especially, due to the main components such as heat exchangers which are relatively big in comparison to the size requirements of the complete system. In addition to that, together the structure of the preliminary prototype and the size of the valves to control the air flows for the adsorption and desorption were misleading. The first design of the whole construction became possible after finding a solution for the key question to control adsorption and desorption phases effectively by one active valve. Hence, this simple valve mechanism continued as a fulcrum through the whole design.

Apart from the structure, it was important in the beginning to clarify informative efficiencies and the total energy allocation of such a multiple power source device. This clarification showed that fans are the highest electric power consumers. Therefore, in the beginning the estimations of various fan setups were done to find out if there is a theoretical possibility to reach the $COP_{electric}$ of 20. After having a general idea about the structure and a positive results from the initial estimations of the power consumptions, it was possible to start the optimization of the functional components.

The optimization started with fans. In the fan optimization new fan technologies with effective housings were applied. The design process continued with an idea to apply an indirect evaporative cooling into the cooling box instead of a direct evaporative cooling. Advantages of the new fan design and the new cooling box compared to the first construction were determined in the second construction. After the second construction, it was important to prove the competitiveness of the valve mechanism, which is one of the main components. In the third and the last stage of the design process, rest of the components, such as filters and water cycles were optimized and applied to the third construction. Finally, the design work ended to the comprehensive pressure loss calculations and the $COP_{electric}$ was precisely defined.

In comparison between the design outcome and the requirement list, all the key requirements are fulfilled. The main requirements are the electric cooling coefficient of performance and the size. Remarkable result is the reached electric cooling coefficient of performance $COP_{electric} \approx 29$ with the structure ($0,8\text{ m} * 0,9\text{ m} * 1,5\text{ m}$) which fairly fits to the size requirements. Additionally, it should be mentioned that, the invention of the valve mechanism can be used in every open cycle and alternating DEC system. The efficiency of the valve mechanism is independent on the size, which is the main advantage in a comparison to the common desiccant wheel. Furthermore, the valve mechanism was experienced useful and it led to the invention report of patent application, which is still under procedure.

Some points from the requirement list are still unattended. For example, noise level clarifications, maintenance possibilities and specific connections to the domestic hot water system were excluded. Although, that these points are missing explicitly, they were kept in mind through whole design, and hence the implementation is possible during further development. According to the desired design outcome, manufacturing costs and comparison between solutions were also left out. A reasonable manufacturing cost calculation was not conclusive at this state of the project. Regarding the valve mechanism in the background of the construction, all structural solutions followed the same general idea, thus comparison between the three solutions is unreasonable. In addition to that, the percentage of pressure loss which is due to the structure is low, and therefore

the sizes of the functional components are primarily defining the minimum size. Hence, more precise structure optimizations of the device can offer only insignificant advantages compared the design in this thesis.

The results obtained in this thesis are strongly supporting a further development of the presented desiccant evaporative cooling system for detached house use. To design an actual product extensive design work has to be conducted out and much development and experimental design has to be done. First, the sheet metal structure has to be designed, and then the functional components can be carried to the detailed level. After that, piping, wiring and sensors has to be designed and the needed functions of the control unit can be defined. Then, factors such as producibility, maintenance and the real performance should be proven in practice. Finally, concentration should be on the manufacturing costs. The system contains several customized components and a precise research to the suppliers and to the manufacturing methods would offer significant advantage. This thesis, however has proven the competitiveness of the system and gives general guidelines and ideas for the further design of such a system, which probably will be applied to zero-energy houses in the future.

REFERENCES

- 2008 ASHRAE handbook. 2008. Heating, ventilating and air-conditioning systems and equipment, SI edition. ASHRAE, Atlanta.
- 2009 ASHRAE handbook. 2009. Fundamentals, SI edition. ASHRAE, Atlanta.
- Advancing the science of climate change. 2010. America's Climate Choices: Panel on Advancing the Science of Climate Change National Research Council. National Academies Press, Washington D.C.
- Aerastar. n.d. Junkers, bosch thermotechnik gmbh. Product document. Quoted 16.3.2011. http://www.junkers.com/de/pmdb/brochures/L%C3%BCftung_-_Aerastar.pdf.
- Böckh, P. v. 2006. Wärmeübertragung: Grundlagen und Praxis, 2nd edition. Springer, Berlin, Heidelberg, New York.
- Bosch Today. 2010. The Bosch Group corporate presentation. Robert Bosch GmGH, Stuttgart. Quoted 7.3.2011.
- Çengel, Y. A. 2008. Fundamentals of thermal-fluid sciences, 3rd edition. McGraw-Hill, Boston.
- Davies, C. N. 1952. The Separation of Airborne Dust and Particles. Proceedings of the Institution of Mechanical Engineers (SAUS), London.
- DIN 1946-2. 1994. Raumlufttechnik Teil 2- Gesundheitstechnische Anforderungen. Standard. Deutsches Institut für Normung. Beuth, Berlin.
- DIN 1946-6. 2009. Raumlufttechnik – Teil 6: Lüftung von Wohnungen – Allgemeine Anforderungen, Anforderungen zur Bemessung, Ausführung und Kennzeichnung, übergabe/übernahme(Abnahme) und Instandhaltung. Standard. Deutsches Institut für Normung. Beuth, Berlin.
- DIN EN 13779. 2007. Lüftung von Nichtwohngebäuden – Allgemeine Grundlagen und Anforderungen für Lüftungs- und Klimaanlageanlagen und Raumkühlsysteme. Standard. Deutsches Institut für Normung. Beuth, Berlin.
- DIN EN 779. 2009. Partikel-Luftfilter für die allgemeine Raumlufttechnik - Bestimmung der Filterleistung. Standard. Deutsches Institut für Normung. Beuth, Berlin.
- Directive 2010/31/EU. 2010. the European Parliament and of the Council. 19 May 2010 on the energy performance of buildings. The European Parliament and of the Council. Quoted 3.3.2011. <http://eur-lex.europa.eu/LexUriServ/LexUriServ.do?uri=OJ:L:2010:153:0013:0035:EN:PDF>.
- Eck, M. 2008. Solartechnik - Hochtemperatureanwendungen 2: Einführung in die solare Strahlung. Handout. Stuttgart Universität. DLR Institut für Technische Thermodynamik, Stuttgart.

- Ensor, D. and Donovan, R. 1988. Handbook of contamination control in microelectronics: Principles, applications and technology, edited by Tolliver, D. L. Noyes Publications, New Jersey.
- Exzenter Hohlkegeldüsen. n.d. Lechler GmbH. Baureihe 302 product document. Quoted 15.4.2011. https://shop.lechler.de/is-bin/intershop.static/WFS/LechlerDE-Shop-Site/LechlerDE-Shop/de_DE/PDF/industrie/deutsch/Hohlkegelduesen_Lechler_DE.pdf.
- Facts and Figures. 2011. The Bosch Group corporate presentation. Robert Bosch GmbH, Stuttgart. Quoted 7.3.2011.
- Grote, K.-H. and Feldhusen, J. 2007. Dubbel: Taschenbuch für den Maschinenbau, 22nd edition. Springer, Berlin, New York.
- Grundfos ALPHA2. n.d. Grundfos AB. Product document. Quoted 15.4.2011. <http://net.grundfos.com/Appl/WebCAPS/ProductDetailCtrl?cmd=com.grundfos.webcaps.productdetail.commands.ProductDetailCommand&productnumber=95047526&freq=50&page=0&selectedRow=0>.
- Hämäläinen, J. and Järvinen, J. 2006. Elementtimenetelmä virtauslaskennassa, 2nd edition. Tieteen tietotekniikan keskus CSC. Quoted 14.2.2011. CSC - Tieteellinen laskenta Oy, Espoo. <http://www.csc.fi/downloadPublication?uid=fd6b5e0d1158131358a5f7ff991373c0>.
- Henning, H.-M. 2004. Solar-assisted air-conditioning in buildings: A handbook for planners. International Energy Agency. Springer, Wien, New York.
- Henning, H.-M. 2009. Kühlen und Klimatisieren mit Wärme. Solarpraxis, Berlin.
- Incropera, F. P. and DeWitt, D. P. 1996. Fundamentals of heat and mass transfer, 4th edition. Wiley, New York.
- Kast, W. 1988. Adsorption aus der Gasphase: Ingenieurwissenschaftliche Grundlagen und technische Verfahren. VCH, Weinheim.
- Key World Energy Statistics 2010. 2010. International Energy Agency (IEA). International Energy Agency, Paris. Quoted 3.3.2011. http://www.iea.org/textbase/nppdf/free/2010/key_stats_2010.pdf.
- Knies, G. DESERTEC Foundation. Quoted 3.3.2011. <http://www.desertec.org/>.
- Korhonen, H. and Lintunen, M. 2003. The good indoor air. Like Publishing Ltd., Helsinki.
- Kübler, H. 2010. Messtechnische Untersuchung eines Prototypen zur Solaren Klimatisierung. Master's thesis. Hochschule für Angewandte Wissenschaften Hamburg, Department Maschinenbau und Produktion.
- Langmuir, I. 1916. The evaporation, condensation and reflection of molecules and the mechanism of adsorption. *Physical Review*, 8:149–176.
- Linear actuator CAR 22. n.d. SKF Group. Product document. Quoted 6.4.2011. <http://www.skf.com/medialibrary/asset/0901d1968009e1db>.
- Luukkanen, P. 2001. Pumpunvalitsimet integroidussa simulointiympäristössä. Master's thesis. Lappeenrannan teknillinen korkeakoulu, Kemianteekniikka.

Ng, K. C., Chua, H. T., Chung, C. Y., Loke, C. H., Kashiwagi, T., Akisawa, A., and Saha, B. B. 2001. Experimental investigation of the silica gel-water adsorption isotherm characteristics. *Applied Thermal Engineering*, 21(16th):1631–1642.

Oertel, K. 2001. *Adsorberwärmeübertrager zur Kälteerzeugung mit Niedertemperaturwärme*. VDI-Verlag, Düsseldorf.

Planning and installing solar thermal systems. 2010. A guide for installers, architects and engineers, 2nd edition. The German Solar Energy Society (DSG). Earthscan, London.

Radialventilatoren/Katalog. n.d. Ebm-papst GmbH & Co. KG. Product document. Quoted 22.3.2011. http://www.ebmpapst.com/media/content/info-center/downloads_10/catalogs/centrifugal_fans_1/Radialventilatoren_2007_-DE.pdf.

Robert Bosch: His life and work. 2011. *Journal of Bosch History*. Supplement 1. Robert Bosch GmbH, Stuttgart. Quoted 3.3.2011. http://www.bosch.com/content/language1/downloads/SH1-07_en_aktuell.pdf.

RS160. n.d. Recair B.V. Product document. Quoted 8.2.2011. http://www.recair.nl/docs/file/Recair_Sensitive_RS1_2B0D2B.pdf.

SFP-opas. 2009. LVI-talotekniikkateollisuus ry. Quoted 17.3.2011. <http://www.flaktwoods.fi/476d6be3-be6e-42e9-bd82-6152ff71a7aa>.

Siikonen, T. 2010. *Virtaussimulointi*. Helsinki University of Technology, Helsinki.

Sisäilmastoluokitus 2008. 2008. *Sisäympäristön tavoitearvot, suunnitteluohjeet ja tuotevaatimukset*. Sisäilmayhdistys, Espoo.

Status of Ratification of the Kyoto Protocol. 2011. United Nations Framework Convention on Climate Change. Quoted 11.3.2011. http://unfccc.int/kyoto_protocol/status_of_ratification/items/2613.php.

Vallox ilmanvaihtokoneet. n.d. Vallox Oy. Product document. Quoted 8.2.2011. <http://www.vallox.com/tuotteet>.

Vastavirtakennoiset ilmanvaihtolaitteet. n.d. Oy Swegon AB. Product document. Quoted 8.2.2011. <http://www.swegon.com/fi/Tuotteet/Asuntoilmanvaihto/Ilmanvaihtolaitteet/Tulo-ja-poistoilmalaitteet-lammontalteenotolla/Vastavirtakennoiset-W-sarja/>.

Very fast-running actuators. n.d. BELIMO Automation AG. Product document. Quoted 7.4.2011. <http://www.belimo.eu/CH/EN/Product/Actuators/Product-Detail.cfm?MatNr=NMQ24A&CatNr=0206030101&>.

Weather Information for Rome (ROMA). 2011. World Weather Information Service. World Meteorological Organization. Quoted 3.3.2011. <http://www.worldweather.org/176/c00201.htm>.

Weinmann, R. 2011. Ebm-papst GmbH & Co. KG representative. Meeting 24.2.2011.

White, F. M. 2003. *Fluid mechanics*, 4th edition. McGraw-Hill, Boston.

APPENDICES

Appendix 1. Requirement list

[Material deleted due to confidentiality]

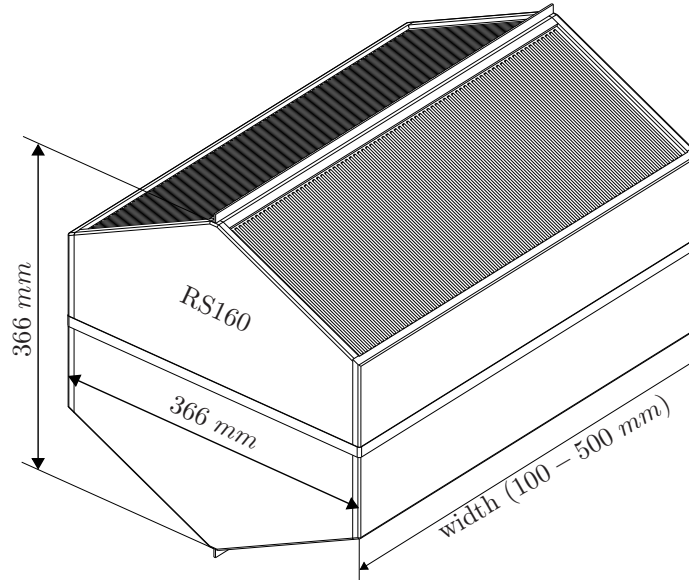
[Material deleted due to confidentiality]

Appendix 2. Coated heat exchangers

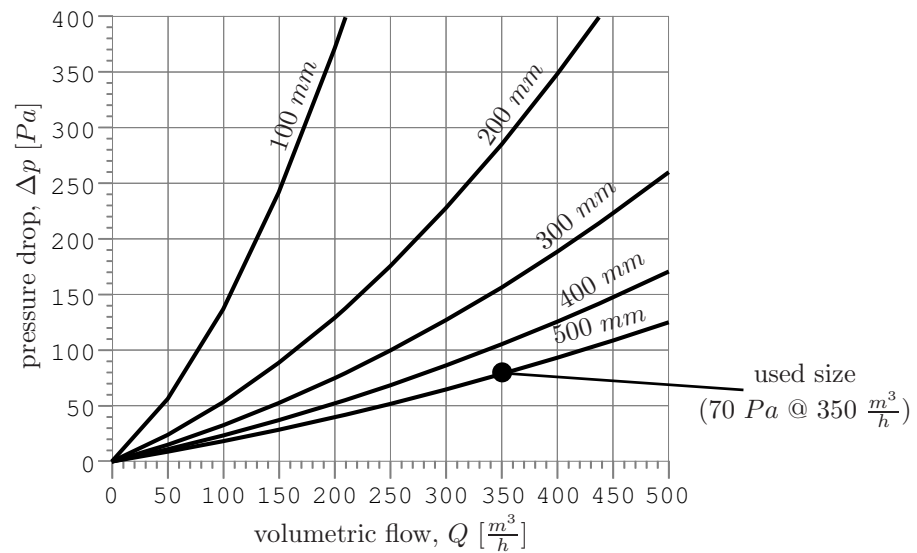
[Material deleted due to confidentiality]

Appendix 3. Cross counter flow heat exchanger

Recommended cross counter flow heat exchanger for IEC use is Recair RS160 (according to RS160, nd):



Dry air pressure loss for one direction as a function of volumetric flow in Recair RS160 with standard widths (100-500 mm)(according to RS160, nd):



Given values are valid only for dry air:

⇒ Supply air is dry and pressure drop is 70 Pa

Water is sprayed to discharged air and pressure drop is more in the wet side:

⇒ According to experimental tests with prototypes, discharged air pressure drop is 90 Pa

Appendix 4. Efficiency estimations

[Material deleted due to confidentiality]

Appendix 5. Initial setup possibilities

[Material deleted due to confidentiality]

Appendix 6. Competitors technical data

Product data from the competitors brochures:

Product	Standard/ maximum flow [m^3/h]	Standard/ maximum power [W]	External pressure [Pa]	Connections [$n * \varnothing mm$]
Junkers AERASTAR LP150 ^a	170/220	63/130	150	4*125
Junkers AERASTAR LP250 ^a	210/300	98/150	150	4*160
Junkers AERASTAR LP350 ^a	340/400	160/260	150	4*160
Vallox 90 SE (DC) ^b	182/331	50/173	50	4*125
Vallox 121 SE (DC) ^b	210/382	63/224	100	6*125
Vallox 150 SE (DC) ^b	289/526	90/340	100	4*200
Vallox 180 SE (DC) ^b	350/637	116/415	100	4*200
Swegon CASA W100 Premium ^c	175/360	75/238	100	4*160
Swegon CASA W130 Premium ^c	216/468	125/340	175	4*160

^a(Aerastar, nd)

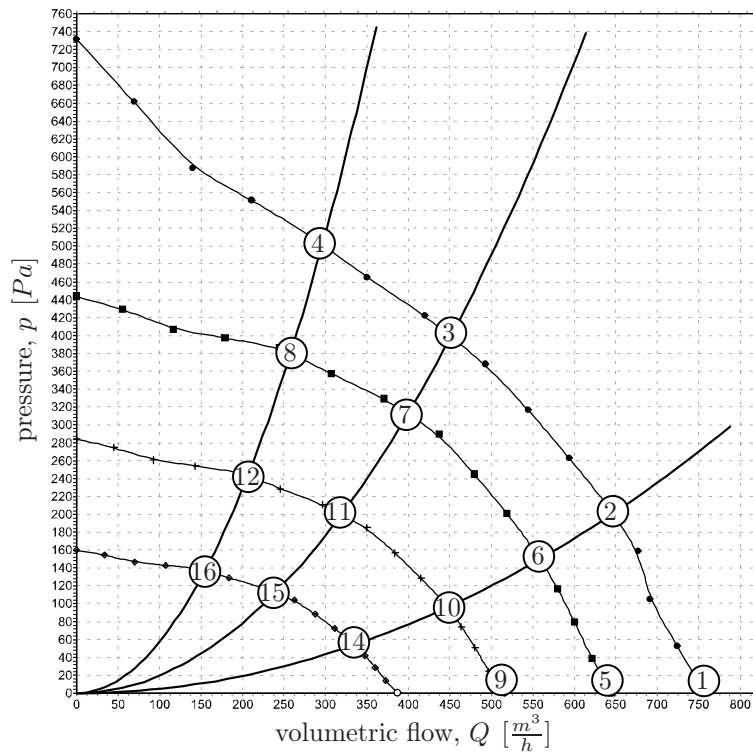
^b(Vallox ilmanvaihtokoneet, nd)

^c(Vastavirtakennoiset ilmanvaihtolaitteet, nd)

Appendix 7. RadiCal fans

[Material deleted due to confidentiality]

Fan curves of the RadiCal fan R3G190RG2303 (Weinmann, 2011).



Measured values of the RadiCal fan R3G190RG2303 in operating points (Weinmann, 2011).

#	U [V]	f [Hz]	n [$\frac{1}{min}$]	P [W]	I [A]	L_p [dB(A)]	Q [$\frac{m^3}{h}$]	p [Pa]
1	230	50	3520	88	0,63	70	755	0
2	230	50	3470	93	0,67	63	645	200
3	230	50	3375	96	0,80	58	450	400
4	230	50	3445	94	0,68	63	295	500
5	230	50	3000	55	0,39	66	645	0
6	230	50	3000	60	0,43	59	560	150
7	230	50	3000	68	0,49	55	400	312
8	230	50	3000	62	0,45	60	260	380
9	230	50	2400	28	0,20	62	515	0
10	230	50	2400	31	0,22	55	445	96
11	230	50	2400	35	0,25	50	320	200
12	230	50	2400	32	0,23	55	205	244
13	230	50	1800	12	0,08	55	385	0
14	230	50	1800	13	0,09	48	335	54
15	230	50	1800	15	0,11	44	240	112
16	230	50	1800	13	0,10	49	155	137

Reached efficiency with the RadiCal fans:

[Material deleted due to confidentiality]

Appendix 8. Beam torque optimization

[Material deleted due to confidentiality]

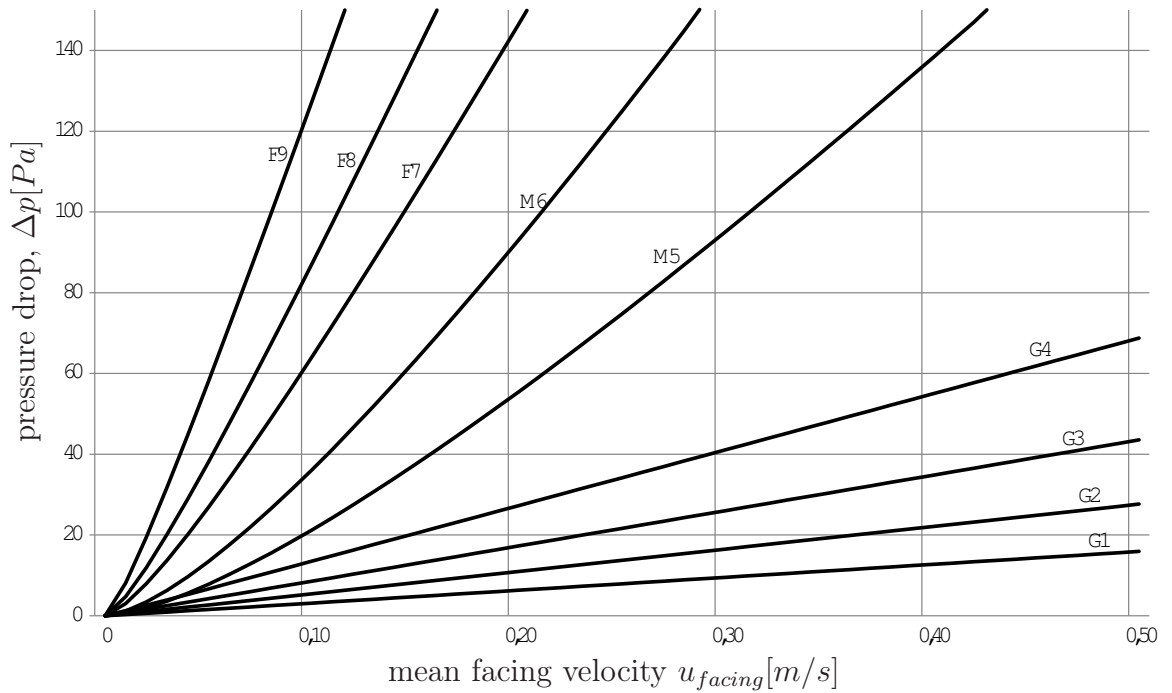
[Material deleted due to confidentiality]

Appendix 9. Beam thickness optimization

[Material deleted due to confidentiality]

[Material deleted due to confidentiality]

Appendix 10. Pressure drop in fibrous filters



Pressure drop in fibrous filters as a function of mean facing velocity. Filters are classified and values are calculated according to the requirements given in standard DIN 779.

In the filter calculations, the equations are given by (Ensor and Donovan, 1988):

α_{filter} =the solidity of the filter, normally in fibrous filters 5 – 6 %

$d_{particle}$ =the diameter of the particle wanted to be filtered, 0,4 μm (DIN EN 779, 2009, p. 12)

d_{fiber} =the diameter of a single fiber, in fine glass fiber filters 0,5 – 5 μm

Z_{filter} =the thickness of the filter, 0,30 – 0,75 mm according to the filter manufacturers

u_{facing} =the mean facing velocity between air flow and filter

Efficiency of a single fiber is given by:

$$\eta_{fiber} = \eta_d + \eta_{d,i} + \eta_i$$

Effect of the diffusion is given by:

$$\eta_d = 2,9 * Ku^{-\frac{1}{3}} * Pe^{-\frac{2}{3}} + \frac{0,624}{Pe}$$

Where the Kuwabara number is:

$$Ku = -0,75 - \frac{1}{2} * \ln \alpha_{filter} + \alpha_{filter} - 0,25 * \alpha_{filter}^2$$

And the Peclet number is:

$$Pe = \frac{d_{fiber} * u_{facing}}{D}$$

The diffusion coefficient is defined by:

$$D = \frac{k_B * \vartheta * C}{3 * \pi * \mu_{air} * d_{particle}}$$

Where k_B is the Boltzmann's constant and the Cunningham slip correction factor is:

$$C = 1 + \frac{2,468 * \lambda}{d_{particle}} + \frac{0,826 * \lambda}{d_{particle}} * \exp\left(-\frac{0,425 * d_{particle}}{\lambda}\right)$$

The mean free path of air molecule is:

$$\lambda = \frac{\mu_{air}}{\rho_{air}} * \sqrt{\frac{\pi * M_{air}}{2 * k_B * \vartheta_{air}}} \text{ in STP conditions } \lambda = 66 \text{ nm}$$

The effect of the diffusion-interception is given by:

$$\eta_{d,i} = 1,24 * \sqrt{\frac{1}{Ku}} * \sqrt{\frac{1}{Pe}} * \sqrt[2]{R}$$

Where the interception parameter is:

$$R = \frac{d_{particle}}{d_{fiber}}$$

The effect of the interception is given by:

$$\eta_i = \frac{1}{2 * Ku} * \left(2 * (1 + R) * \ln(1 + R) - (1 + R) + \frac{1}{1 + R}\right)$$

The efficiency of the whole filter is:

$$\eta_{filter} = 1 - \exp\left(\frac{4 * \alpha_{filter} * \eta_{fiber} * Z}{\pi * d_{fiber} * (1 - \alpha_{filter})}\right)$$

To keep the efficiency constant with all mean facing velocities, the thickness is changing:

$$\Rightarrow Z = \ln(1 - \eta_{filter}) * \frac{\pi * d_{fiber} * (1 - \alpha_{filter})}{4 * \alpha_{filter} * \eta_{fiber}}$$

The pressure drop in filter is given by:

$$\Delta p = \frac{u_{facing} * Z_{filter} * \mu}{d_{fiber}} * [64 * \alpha_{filter}^{1,5} * (1 - 56 * \alpha_{filter}^3)]$$

Appendix 11. Water cycles

[Material deleted due to confidentiality]

[Material deleted due to confidentiality]

Appendix 12. Pressure loss in cooling box

[Material deleted due to confidentiality]

Appendix 13. Pressure loss in third construction

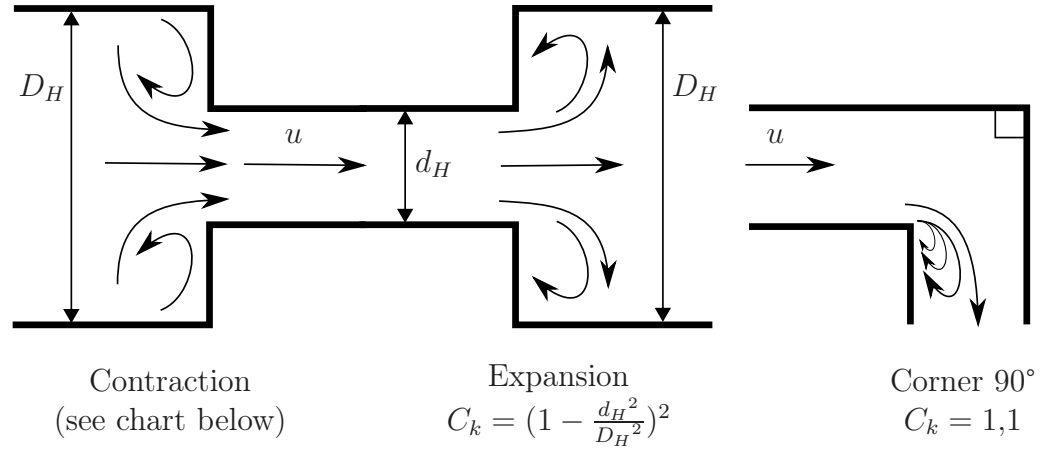
[Material deleted due to confidentiality]

[Material deleted due to confidentiality]

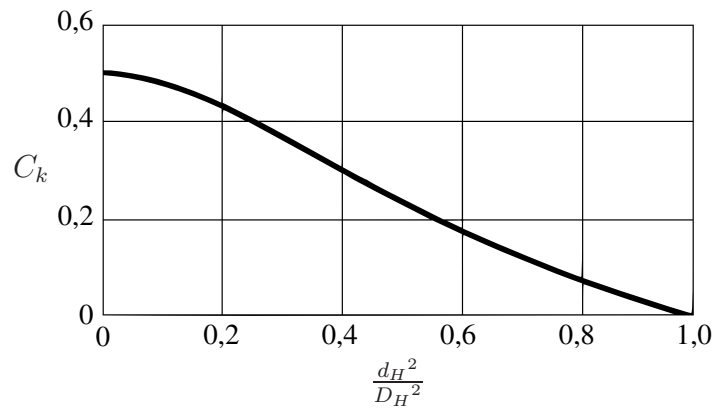
[Material deleted due to confidentiality]

[Material deleted due to confidentiality]

For contraction, expansion and 90° corner C_k is defined by (according to Çengel, 2008, pp. 634-635):



For sudden contraction C_k is given by:



Appendix 14. Computational pressure loss

[Material deleted due to confidentiality]

[Material deleted due to confidentiality]